Electrophysiological and Morphological Properties of Neurons in the Superficial Layer of the Rat Superior Colliculus

Toshiaki Endo

Department of Physiological Science

School of Life Science

The Graduate University for Advanced Studies

CONTENTS

General Introduction

Formation of behavioral responses to visual stimuli is one of the most fundamental processes in the brain and the neuronal mechanisms of the visuo-motor transformation is one of the central issues in the field of brain research. The mammalian superior colliculus (SC) is an essential center controlling visually guided behaviors such as saccadic eye movements, orienting head and body movements and lots of behavioral, physiological and anatomical studies have been concentrated on analysis of function of the SC to study the visuo-motor transformation process therein (for review see Dean et al., 1989; Sparks 1986; Wurtz and Albano 1980). Anatomically, the SC is located on the dorsal side of the midbrain, and roughly divided into three layers: the superficial, intermediate and deep layers. The superficial layer is further divided into three sublayers: the stratum zonale (SZ), the stratum griseum superficiale (SGS) and the stratum opticum (SO). The optic fibers run through the SO, and project to the whole extent of the superficial layer. The superficial layer receives visual input from the retina and the primary visual cortex with topographically organized manner, and in turn sends its output to several regions including the pulvinar and the dorsal lateral geniculate nucleus (dLGN) (Huerta and Harting, 1984). Neurons in the superficial layer of the SC also project to deeper layers of the SC (Isa et al., 1998; Lee et al., 1997; Mooney et al., 1988a). The pathway from the retina, via the superficial layer of the SC and the pulvinar to the extrastriate cortex is called the extrageniculate visual pathway, which is thought to be involved in visual orientation and spatial attention. In contrast, the primary visual pathway which is thought to be involved in visual perception projects to the visual cortex via the dLGN. Anatomical connection described above suggests that the superficial layer of SC is a relay station of the

extrageniculate visual pathway, and at the same time, can also play a significant role in connecting the two visual pathways. Thus, to study the function of the superficial layer of the SC should help us understand the mechanisms of visual processing and attentional systems in the brain.

There have been numerous investigations on visual response properties of neurons in the SC superficial layer (Binns and Salt, 1997; Cynader and Berman, 1972; Goldberg and Wurtz, 1972a,b; Humphrey, 1968; Mooney et al., 1985, 1988; Schiller and Koener, 1971). Neurons in the superficial layer of the SC respond to visual stimuli presented in the contralateral visual field. The visual receptive fields have inhibitory surround: presentation of visual stimuli in the surround suppress the neuronal activity. Furthermore, the responses become habituated when same visual stimuli are presented repeatedly. In addition to these most fundamental properties, the responses of visual neurons are known to be modulated dynamically by arousal and attentional level of the animal. For example, the visual responses were enhanced when the animal have to make saccades to the visual stimuli.

To elucidate the neural mechanisms underlying the information processing in the superficial layer of the SC, it is essential to know the fundamental properties of individual neurons composing the local circuits and their mutual interactions in the local circuit. However, while the morphological characteristics of individual neurons in the SC superficial layer have been investigated in numerous anatomical studies, the electrophysiological properties of the morphologically identified neurons have not been studied as yet (Langer and Lund, 1974; Tokunaga and Otani, 1976; Labriola and Laemle, 1977). Recently, Lo et al. (1998) investigated electrophysiological and morphological properties of neurons in the SO using rat slice preparations. However, their study is restricted to that of the

neurons in the SO, and fundamental properties of individual neurons in the other layers (SZ and SZ) have still been unknown.

In this study, we investigated the electrophysiological properties and morphological characteristics of neurons in the whole extent of the superficial layer of rat SC including SZ, SGS and SO, using whole-cell patch clamp recording technique. We have focused on the three points: 1) membrane properties revealed by response to depolarizing and hyperpolarizing current pulses and ion conductances involved in expression of the characteristic membrane properties (chapter I), 2) the organization of excitatory synapses, especially on expression of functionally different subtypes of AMPA-type glutamate receptors (chapter II) and 3) the organization of the inhibitory synapses, especially on action of $GABA_B$ receptors (chapter III). The findings of this study will add fundamental knowledge about the dynamic properties of visual processing in the SC.

Chapter I

Intrinsic Electrophysiological Properties of Morphologically Different Subclasses of Neurons

Summary

We investigated electrophysiological and morphological properties of neurons in the superficial layer of the rat superior colliculus (SC) , using whole-cell patch clamp technique in slices obtained from 17- to 21-day old rats. According to the firing responses to depolarizing current pulses, the neurons in the superficial layer (n=262) were classified into six classes: (1) Burst spiking neurons (n=87), these neurons showed transient burst spikes at their firing threshold. (2) Regular spiking neurons (n=131), these neurons generated successive spikes with constant interspike intervals. (3) Late spiking neurons (n=20), the onset of spike generation was remarkably delayed. (4) Fast spiking neurons (n=9), these neurons sustained high-frequency (more than 100Hz) repetitive firing throughout the depolarizing pulse. (5) Neurons with rapid spike inactivation (n=11), spike amplitude was rapidly reduced, and only a few spikes were generated during a prolonged depolarizing current pulses. (6) Neurons with short spike train (n=4), several full-sized spikes were generated, however, spike generation was terminated during initial phase of the depolarizing pulses. Majority of recorded neurons were classified either into type (1) or type (2). In response to hyperpolarizing current pulses, two different types of inward rectification were observed: time-dependent inward rectification ("voltage sag", n=120) caused by hyperpolarization-activated current (I_h) and time-independent inward rectification (n=66) caused by inward rectifier potassium channels. Based on the somatodendritic morphology, the neurons visualized by intracellular staining with biocytin and/or lucifer yellow (n=98) were classified into seven groups following previous descriptions: (a) marginal cells (n=6), (b) narrow field vertical cells (n=15), (c) piriform cells (n=14), (d) horizontal cells (n=18), (e) stellate cells (n=9), (f) wide field multipolar cells

(n=8), and (g) wide field vertical cells (n=28). In general, each groups were heterogeneous with respect to electrophysiological properties among which, however, burst spiking and regular spiking neurons consisted the majority. A notable correlation between morphology and electrophysiological properties was that all type (g) neurons showed marked time-dependent inward rectification by I_h. Voltage clamp analysis revealed that in response to voltage pulses from –50 to –100mV, type (g) neurons expressed I_h with faster activation kinetics (τ =131±11msec, mean ± S.E.) and larger current density (10.5 ± 1.3pA/pF) than the other subclasses (τ =348 ± 31 msec, 2.6 ± 0.4 pA/pF). These results indicated the local circuits of the SC superficial layer include wide variety of neurons with respect to electrophysiological and morphological characteristics, and there seemed to be no specific relationship between their firing properties and morphological cell classification as has been established in other regions in the brain, such as neocortex, hippocampus and striatum, except for specific expression of large and fast I_h in wide field vertical cells.

Introduction

A number of studies using Golgi staining or intracellular staining techniques have demonstrated that there are several morphologically different types of neurons in the superficial layer of the SC (Langer and Lund, 1974; Tokunaga and Otani, 1976; Labriola and Laemle, 1977; Mooney et al., 1985; Moschovakis et al., 1988a,b). For example, in rats, Langer and Lund (1974) described six types of neurons. Tokunaga and Otani (1976) also divided SC superficial layer neurons in a similar manner, although their nomenclature was different.

In contrast to accumulating information about the morphological characteristics of neurons in the SC superficial layer, very little is known about their electrophysiological properties. To elucidate the fundamental mechanisms of information processing in the superficial layer of the SC, it is also essential to understand the intrinsic membrane properties and their underlying membrane conductances of individual neurons composing the local circuits, in addition to the information about their morphological characteristics. Recently, Lo et al. (1998) investigated electrophysiological and morphological properties of neurons in the SO using rat slice preparations. However, their study is restricted to that of the neurons in the SO, and fundamental properties of individual neurons in the other layers (SZ and SZ) have still been unknown.

In the present study, we investigated the electrophysiological properties and morphological characteristics of neurons in the SC superficial layer including SZ, SGS and SO, using whole-cell patch clamp technique. In the cerebral cortex, hippocampus and other structures in the brain, characteristic relationship between the electrophysiological properties and morphology of the cells has been described (McCormick et al, 1985; Connors

and Guttnick, 1990; Kawaguchi et al., 1987; Kawaguchi and Kubota, 1997). We examined whether the findings established in the other parts of the brain fit in the superficial layer of the SC. Our laboratory has recently analyzed the electrophysiological and morphological properties of neurons in the intermediate layer, which generate motor output from the SC (Saito and Isa 1999). Comparison of neural elements in both layers will be discussed in discussion and reveal characteristics of neuron circuits of the superficial layer dedicated to sensory processing rather than shaping of the motor command as is processed in the intermediate layer..

Methods

Slice preparation

Frontal slices (250–400μm thick) of the SC were prepared from 17- to 21-day-old Wistar rats. The animals were deeply anesthetized with ether and decapitated. The brains were quickly removed and submerged in the ice-cold modified Ringers' solution containing (mM) : 234 sucrose, 2.5 KCl, 1.25 NaH_2PO_4, 10 $MgSO_4$, 0.5 $CaCl_2$, 26 $NaHCO_3$, 11 glucose and bubbled with 95% O_2 and 5% CO_2 for 5–10 minutes. Then slices were cut with a Microslicer (DTK-2000, Dosaka EM, Kyoto, Japan), and they were incubated in control Ringer's solution at room temperature for > 1 hour before recording. The control Ringers' solution contained (mM) : 125 NaCl, 2.5 KCl, 2 $CaCl_2$, 1 $MgCl_2$, 26 $NaHCO_3$, 1.25 NaH_2PO_4, 25 glucose, and was bubbled with 95% O_2 and 5% CO_2 (pH 7.4).

Whole-cell patch clamp recording

A slice was mounted in a recording chamber on an upright microscope (Axioskop FS, Zeiss, Germany or DM LFS, Leica, Germany), and neurons were visualized with Nomarski optics. Whole-cell patch clamp recordings (Edwards et al. 1989; Hamill et al. 1981) were obtained from randomly selected neurons using an EPC-7 or EPC-9 patch clamp amplifier (HEKA, Lambrecht, Germany). Patch pipettes were prepared from borosilicate glass capillaries (GC150F-15 or -10, Clark Electromedical Instruments, Pangbourne, England) with a micropipette puller (P-97, Sutter Instrument Co., Novato, CA). The slice was continuously superfused with control Ringers' solution by a peristalic pump (Minipuls 3, Gilson, Villiers, France). For voltage-clamp analysis of activation kinetics of inward rectifier current, the Ringer's solution contained (mM) : 145 NaCl, 2.5 KCl, 2$CaCl_2$, 1 $MgCl_2$, 5

HEPES, 10 glucose, and continuously bubbled with 100% O_2 (pH 7.4). HEPES buffer was used so that we could add Cd^{2+} in the solution to block the voltage-dependent Ca^{2+} channels for succeeding experiment, but present data were obtained under Cd^{2+}-free condition. Intracellular solution contained (mM) : 140 K-gluconate, 20 KCl, 0.2 EGTA, 2 $MgCl_2$, 2 Na_2ATP, 10 HEPES, 0.1 spermine, pH 7.3. To stain the recorded neurons, biocytin (5 mg/ml, Sigma, St. Louis, MO) was dissolved in the solution. In some cases, lucifer yellow (1 mg/ml, Sigma) was also dissolved in the solution. The resistance of the electrodes was 3–8MΩ in the Ringer's solutions. All recordings were performed at room temperature (22–25℃). Data were acquired by pClamp system (Axon Instruments, Inc., Foster City, CA) or software PULSE (HEKA). The input resistance of each neuron was calculated from the voltage change induced by hyperpolarizing current pulse (typically, –40pA) from the membrane potential of –55 to –70mV.

Histological procedure

After recording, the slices were fixed with 4% paraformaldehyde in 0.12M phosphate buffer (pH 7.4) for more than a day at 4℃. After fixation, lucifer yellow-filled neurons were photographed using epifluorescent microscope (Axioplan 2, Zeiss). Biocytin-filled neurons were visualized by staining with biocytin (Horikawa and Armstrong, 1988). The slices were rinsed in 0.05M phosphate-buffered saline (PBS, pH 7.4) several times, and then incubated in methanol containing 0.6% H_2O_2 for 30 min. After rinsed with PBS, the slices were incubated in PBS containing 1 % avidin-biotin peroxidase complex (Vector Laboratories) and 0.3% Triton-X100 for 3 hours. After washes with PBS and then 0.05M Tris-buffered saline (TBS, pH 7.6), the slices were incubated in TBS containing 0.01% diaminobenzidine tetrahydrochloride, 1% nickel ammonium sulfate, and 0.0003% H_2O_2 for 30

min. All procedures were performed at room temperature. The slices were mounted on gelatin-coated slides, counterstained with cresyl violet, dehydrated and coverslipped. In some cases, the slices were incubated in PBS containing 2% gelatin for 2 min before mounted on gelatin-coated slides.

The morphological profiles of stained neurons were drawn using camera lucida attached to a light microscope.

Results

Firing responses to depolarizing current pulses

We recorded voltage responses to depolarizing current pulses (in most cases, up to 200pA in 40pA step, 400ms duration) in 262 neurons, and classified them into six classes according to their firing properties. Depolarizing current pulses were routinely applied from two different membrane potentials; –50 ~ –65 mV (depolarized membrane potentials) and –70~ –90 mV (hyperpolarized membrane potentials) by varying the intensity of constantly injected currents. Firing properties of the recorded cells were classified according to the firing responses from the hyperpolarized membrane potentials, since difference in firing responses became manifest only in this protocol as will be described below. Neurons with resting membrane potential more negative than –50mV and overshooting spikes were used for analysis. Majority of recorded neurons were classified into either "burst spiking neurons" or "regular spiking neurons".

Burst spiking neurons

Figure I-1A–C shows an example of burst spiking neurons. In response to depolarizing current pulses, the neuron showed transient burst of more than two spikes (Fig. I-1A and B) followed by prominent afterdepolarization (Fig. I-1B, arrowhead). These burst firings appeared with all-or-non manner at firing threshold (Fig. I-1B). The burst firing was observed only when the current pulses was injected from relatively hyperpolarized membrane potential (in this case, –78mV, Fig. I-1A and B). When the current pulse was applied at more depolarized level (–60mV), the burst firing disappeared (Fig. I-1C) and the firing occurred at more regular intervals. Thirty-three percentage (87/262) of recorded neurons showed this

type of firing.

We tested the effect of low concentration of Ni^{2+} on transient burst firing in 3 cells. When 0.5 mM Ni^{2+} was applied to the extracellular solution, the burst firing was inhibited (Fig. I-1D and E), and recovery was observed with wash out (data not shown). This sensitivity to low concentration of Ni^{2+}, voltage dependency of appearance of burst firing and transient nature of the burst suggest that low-threshold Ca^{2+}-channels contribute to the burst firing.

Regular spiking neuron

Figure I-2 shows an example of regular spiking neurons. In response to depolarizing current pulses, the neuron generated successive solitary spikes at constant intervals (Fig. I-2A). The observation was confirmed when the depolarizing current pulses were applied from both the depolarized and hyperpolarized membrane potentials. Although some neurons generated spikes with rigidly constant firing frequency, a majority of neurons belonging to this group showed moderate spike frequency adaptation as shown in figure I-2B. Fifty percentage (131/207) of recorded neurons were classified into this class.

Other neurons

Majority (83%) of neurons recorded in the superficial layer were classified into either burst spiking or regular spiking neurons, however, remaining small number of neurons included another four classes of neurons: late spiking neurons, fast spiking neurons, neurons with rapid spike inactivation, and neurons with short spike train.

Eight percentage (20/262) of neurons were classified into late spiking neurons. Figure I-3A exemplifies a neuron of this class. In this neurons,

generation of the first spike was markedly delayed when depolarizing current pulses were injected from the hyperpolarized membrane potential (–87mV). A small hyperpolarizing deflection was observed just after the initial depolarization induced by the current pulse (arrowhead in Fig. I-3A). This delay disappeared when current pulse was injected from more depolarized level (–68mV). Three percentage (9/262) of neurons were classified into fast spiking neurons and figure I-3B exemplifies a neuron in this class. These neurons showed sustained high-frequency repetitive firing throughout the depolarizing pulses. The neurons classified into this class showed repetitive and stable firing with more than 100Hz with virtually no spike frequency adaptation in response to current pulses up to 200pA. Four percentage (11/262) of neurons were classified into neurons with rapid spike inactivation (Fig. I-3C). Spike amplitude decreased rapidly, spike width became larger and larger, and spike train was terminated after only a few spikes were generated, even when the membrane potential was held above the threshold level. Two percentage (4/262) neurons were classified into neurons with short spike train. When current pulses were injected into these neurons, several full-size spikes were generated, but spike generation was suddenly terminated within 200ms after onset of current injection.

Responses to hyperpolarizing current pulses

We recorded voltage responses to hyperpolarizing current pulses from 251 neurons among the 262 neurons described above. Forty-eight percentage of these neurons (120/251) showed marked time-dependent inward rectification. Figure I-4 shows examples of time-dependent inward rectification. In response to hyperpolarizing current pulses, the membrane potential was gradually re-depolarized following initial hyperpolarization, showing "voltage sag" (Fig. I-4A1). In voltage clamp recording, slowly

developing inward currents were observed in response to hyperpolarizing voltage pulses (Fig. I-4B1). This slow activation kinetics was reminiscent of hyperpolarization-activated current (I_h). Consistent with this idea, ZD7288, which selectively inhibit I_h (BoSmith et al., 1993; Harris and Constanti, 1995), effectively inhibited time-dependent inward rectification with a concentration of 100 μM (n=8, Fig. I-A–D). Furthermore, time-dependent inward rectifier currents were inhibited by 3 mM Cs^+ (n=7, Fig. I-E) but was resistant to 0.5 mM Ba^{2+} (n=6, Fig. I-F), consisting with known properties of I_h (Pape, 1996). Among 120 neurons which showed this type of inward rectification, 45 were burst spiking neurons, 61 were regular spiking neurons, and 14 were other types of neurons (see Table I-1).

In another group of neurons, hyperpolarizing current pulses elicited membrane hyperpolarization with a marked decrease in input resistance at more hyperpolarized membrane potential (Fig. I-5A1). In voltage clamp recordings from this neuron, rapidly activating outward current was observed in response to hyperpolarizing voltage steps pulses (Fig. I-5A2). Thus, the inward rectification in this case was time-independent and such inward rectification was observed in 26% of recorded neurons (66/251). Time-independent inward rectifier currents were inhibited by both 3 mM Cs^+ (n=4, Fig. I-5B and C) and 0.5 mM Ba^{2+} (n=3, Fig. I-5D and E), suggesting that time-independent inward rectification was caused by inward rectifier potassium current (Hagiwara and Takahashi, 1974; Standen and Stanfield, 1978). Among neurons which showed this type of inward rectification, 24 were burst spiking neurons, 31 were regular spiking neurons, and 7 were other types of neurons (see Table I-1).

Morphological characteristics and electrophysiological properties

Among 262 neurons in which we could record responses to

depolarizing current pulses, 98 neurons were successfully stained with biocytin and/or lucifer yellow. Thsese neurons were classified into seven types based on their somatodendritic morphology: marginal cells, narrow field vertical cells, piriform cells, horizontal cells, stellate cells, wide field multipolar cells and wide field vertical cells. The classification basically follows that of Langer and Lund (1974) and Tokunaga and Otani (1976). In general, neurons in each groups were heterogeneous with respect to electrophysiological properties. Electrophysiological properties of morphologically identified neurons are described below and summarized in Table I-2.

Marginal cells

Six neurons were classified into marginal cells. Marginal cells were small neurons which projected dendrites in the ventral direction. The somata of these neurons were located just beneath the dorsal surface of the SC, i.e. in the SZ. Their dendritic field were about 50–100μm in dorsoventral direction. We could not observe the axons of these cells.

Four of six marginal cells were regular spiking neurons, and three of them showed time-independent inward rectification (Fig. I-6) and one showed time-dependent inward rectification in response to hyperpolarizing current pulses. Remaining two cells were neurons with short spike train, and one of them was with time-independent inward rectification.

Narrow field vertical cells

Fifteen neurons were classified into narrow field vertical cells. Narrow field vertical cells were bipolar or multipolar neurons which have both dorsally and ventrally oriented dendrites. The dorsoventral and mediolateral length of their dendritic field were about 70–230 μm and

80–370 μm, respectively. This type of neurons were scattered throughout various depth in the SGS, and one cell was found in the SO. Five of ten narrow field vertical cells with stained axons had an axon which projected into region dorsal to or same level with their soma (Fig. I-7A). and two of them also had axon ventral to their soma (Fig. I-7B). Five cells with stained axons possessed an axon which extended and issued collaterals ventral to their soma, and two of them had an axon which reached the stratum griseum intermediale (SGI).

Five narrow field vertical cells were burst spiking neurons. Among them, two showed time-dependent inward rectification and one showed time-independent inward rectification (Fig. I-7A) in response to hyperpolarizing current pulses. Nine cells were regular spiking neurons. Among them, four cells with time-dependent inward rectification, two were with time-independent inward rectification, and three were without rectification properties (Fig. I-7B). Remaining one cell was a late spiking neuron without any rectification properties.

Piriform cells

Fourteen neurons were classified into piriform cells. Piriform cells projected dorsally oriented dendrites from dorsal side of their soma. The mediolateral length of their dendritic field were about 70–140μm. This type of neurons were located in dorsal half of the SGS. We could observe axons of nine cells in this group. Seven cells had an axon which projected to region ventral to their somata, and four of them also had axon collaterals beside their dendritic field and/or soma (Fig. I-8A). One cell had an axon which reached the SGI and three had axon which reached the SO (Fig. I-8B). Two cells extended axons in the mediolateral direction and also had axon collaterals beside their dendritic field.

Eight piriform cells were burst spiking neurons (Fig I-8A). Among them, six cells showed time-dependent inward rectification and one cell showed marked time-independent inward rectification. Three piriform cells were regular spiking neuron(Fig I-8A). One of them showed time-dependent inward rectification. Two were classified into neurons with short spike train and one of them showed time-dependent inward rectification. One was a late spiking neuron with time-dependent inward rectification.

Horizontal cells

Eighteen neurons were classifie d into horizontal cells. Horizontal cells projected very long dendrites in horizontal direction, and their dendritic field were about 350–1000μm in mediolateral direction. Dendrites which extend in dorsoventral direction were occasionally observed, but dendritic field of these cells were longer in horizontal direction. This type of neurons were located in the dorsal half of the SGS and just beneath the dorsal surface of the SC. This type of cells had axon which issued arborizations in the region near their soma and restricted within the SGS and the SZ (Fig. I-9A and B). Only one of eleven cells with stained axons had an axon which reached the SO.

Fourteen horizontal cells were regular spiking neurons. Among them, nine cells showed time-dependent inward rectification (Fig. I-9B) and one showed time-independent inward rectification. Three were burst spiking neurons with time-dependent inward rectification (Fig. I-9A). Remaining one cell was a neuron with rapid spike inactivation which did not show inward rectification.

Stellate cells

Nine neurons were classified into stellate cells. Stellate cells were

relatively small, multipolar neurons. Direction of dendrites had no particular orientation. The dendritic field was less than about 180μm in diameter. This type of neurons were located in the dorsal half of the SGS. Five of six cell with axon stained with biocytin had axon arborizations mainly within and/or beside the dendritic field (Fig. I-10B). One cell had an axon which reached the ventral SO.

Five stellate cells were burst spiking neurons and two of them showed marked time-independent inward rectification (Fig. I-10B). Remaining three stellate cells were regular spiking neurons, one was with time-dependent inward rectification and two was with time-independent inward rectification(Fig. I-10A).

Wide field multipolar cells

Eight neurons were classified into wide field multipolar cells. These neurons were multipolar cells with relatively large dendritic field. The dendritic field was about 290–450μm in diameter. This type of neurons were located in the ventral SGS and the SO. We could observe axons of seven cells in this group. Four cells had axon arborizations within or beside their dendritic field, and two of them also extend collaterals in horizontal direction. One cell had an axon which issued collaterals dorsal to the soma and the axon reached just beneath the dorsal surface of the SC (Fig. I-11B). Two cells extend an axon in ventral direction and the axon reached the SGI.

Five of eight wide field multipolar cells were regular spiking neurons, three of them showed time-independent inward rectification (Fig. I-11B) and one showed time-dependent inward rectification in response to hyperpolarizing current pulses. One cell was a burst spiking neuron with time-independent inward rectification (Fig. I-11B), one was a late spiking neuron without any rectification properties and one was a fast spiking neuron

with time-independent inward rectification.

Wide field vertical cells

Twenty-eight neurons were classified into wide field vertical cells. Wide field vertical cells extended divergent dendrites toward the dorsal surface of the SC, and had wide dendritic field in the horizontal direction. The dendritic field was about 450–1000μm in the mediolateral direction. The somata of these neurons were found in the most ventral SGS and the SO, except for only one cell whose soma was found in the dorsal SGS. Five of six wide field vertical cells with stained axons had an axon which extended ventral to their somata (e.g., Fig. I-12A), three of them also issued collaterals into the region dorsal to or same level with their soma. One had an axon which projected into the region dorsal to or same level with their soma (e.g., Fig. I-12B).

Thirteen of twenty-eight wide field vertical cells showed burst spiking property (Fig. I-12A), and the remaining cells showed regular spiking property in response to depolarizing current pulses (Fig. I-12B). A notable property of neurons in this class was that all neurons showed marked voltage sag caused by time-dependent inward rectification (Fig. I-12A and B).

Activation kinetics of I_h in different types of neurons

In current clamp recording, prominent voltage sag was observed in wide field vertical cells (e.g., Fig. I-12). In contrast, the voltage sag observed in other neuron types was not as prominent, but appeared to be smaller in amplitude and slower in time course than that observed in wide field vertical cells (e.g., Fig. I-9). This observation suggested that difference exists in activation kinetics of the I_h underlying the voltage sag between wide field vertical cells and other cells. For comparison, activation kinetics of I_h between

wide field vertical cells and other cell types was investigated by applying hyperpolarizing voltage steps from –50 to –100 mV in voltage clamp recording. The slowly activating inward currents (I_h) induced in this protocol were fitted with single exponential function, and the time constant and the steady-state current density (steady-state current amplitude was divided by membrane capacitance) were calculated from the function. Figure I-13A shows examples of a wide field vertical cell. The time constant and the steady-state current density of the I_h were 117 msec and 14.4 pA/pF, respectively.. Figure I-13A shows examples of a horizontal cell. The time constant and the steady-state current density of I_h were 378 msec and 1.95 pA/pF, respectively. The average value of time constant and the steady-state current density of I_h in wide field vertical cells (n=14) were 131 ± 11 msec and 10.5 ± 1.3 pA/pF (mean ± S.E.M.), respectively, while the values in non-wide field vertical cells (n=16) were 348 ± 31 msec and 2.6 ± 0.4 pA/pF, respectively. As shown in Figure I- 13C, I_h in wide field vertical cells (filled circles) tended to be distributed in the region of shorter time constant and larger current density, while I_h in other cells (open squares) tend to be distributed in the region of longer time constant and smaller current density. These results suggest that I_h in wide field vertical cells differs from that in other cell types in both the activation kinetics and the current density.

Discussion

Electrophysiological properties

The results of the present study showed that neurons in the superficial layer of the rat SC can be classified into at least six groups according to their firing responses to depolarizing current pulses. A majority of recorded neurons were classified into either burst spiking neurons (33%) or regular spiking neurons (50%). Burst spiking neurons showed transient burst firing at their firing threshold in response to depolarizing current pulses due to activation of low-threshold Ca^{2+} channels, particularly when the pulses were injected at more hyperpolarized level. Regular spiking neurons composed the largest population in the present study. Most neurons classified into this class showed moderate spike frequency adaptation. However, some regular spiking neurons showed more regular firing. Therefore, although we did not divide these neurons furthermore, regular spiking neurons in this study may include a certain range of neurons with different electrophysiological properties. The present results also show that two different types of inward rectification are observed in neurons in the superficial layer of the rat SC. Time-dependent inward rectification was caused by I_h, and time-independent inward rectification were IRK channels.

Neurons with electrophysiological properties similar to those described in this study were also described in the stratum griseum intermediale (SGI) of the rat SC (Saito and Isa, 1999). However, compared to the present study, burst spiking neurons composed smaller population (13% in the SGI and 33 % in the SGS) and late spiking neurons composed larger population (22% in the SGI and 8 % in the SGS) in the SGI. Regular spiking neurons in the SGI tended to show more regular firing than those in this study. Most regular spiking neurons in the present study showed

moderate spike frequency adaptation, resembling those described in the neocortex (Connors and Gutnick, 1990; McCormick et al, 1985). Thus, there are lamina-specificity in the electrophysiological properties of neurons in the SC that may preclude difference in the way of information processing in each layer.

Morphological characteristics and electrophysiological properties

In the present study, we classified neuron in the superficial layer of the rat SC based on their somatodendritic morphology, following previous descriptions (Langer and Lund, 1974; Tokunaga and Otani, 1976). Although each group was heterogeneous with respect to their electrophysiological properties, the present results demonstrate that wide field vertical cells had marked electrophysiological properties. All these neurons showed clear time-dependent inward rectification caused by I_h, and I_h in neurons in this class was lager in current density and faster in activation time course than that in other cell types. Although differences in activation kinetics could be due to difference in amount and distribution of same channels on the somatodendritic membrane of the cell, difference in properties of channels underlying I_h in these neurons could also cause the difference in activation kinetics. It is known that there are diversity of I_h detected in different types of neurons (Pape 1996), and several members in gene family encoding channels underlying I_h have been cloned recently (Gauss et al., 1998; Ludwig et al., 1998; Santoro et al., 1998). The I_h is involved in several aspect of electrophysiological properties of neurons, such as the resting potential, the shaping of firing patterns and the rhythmic oscillations of the membrane potentials (Pape, 1996). Wide field vertical cells may be lateral posterior nucleus (LP, which corresponds to the pulvinar in primate) projecting neurons, suggested from several lines of evidence. Neurons which

project to the LP are located on the SO and ventral most SGS (Donnely et al, 1983; Lane et al, 1993, 1997; Mason and Groos, 1981; Mooney et al, 1988). In hamster SC, Mooney et al (1988b) demonstrated that about one-half of LP projecting neurons identified by antidromic activation were wide field vertical cells, in contrast, only 5 % of neurons which project to the dLGN were wide field vertical cells. Therefore, it is essential to know the electrophysiological properties of the wide field vertical cells for understanding the information processing in the extrageniculate visual pathway (retina–SC–extrastriate cortex), and I_h may play a crucial role to shaping the information processing throughout the pathway.

In contrast to the wide field vertical cells, other morphological subgroups were composed of heterogeneous subpopulation. In the superficial layer of the SC, horizontal, piriform and stellate cells are thought to be GABAergic inhibitory neurons (Mize, 1992). The results of the present study indicates that all these types contained both burst spiking neurons, regular spiking neurons, neurons with time-dependent inward rectification and neurons with time-independent inward rectification. Because other morphological groups also contained neurons with these electrophysiological properties, we could not find any electrophysiological properties specific to inhibitory or excitatory neuron specific properties in the present study. These situations are quite different from the neocortex, where fast spiking neurons and late spiking neurons are specifically found among GABAergic interneurons and pyramidal cells show either regular spiking or burst spiking properties (Connors and Gutnick, 1990; Kawaguchi and Kubota, 1997).

Functional significance of the electophysiological properties of the SC superficial layer neurons

In the present study, majority of recorded neurons were classified into

either burst spiking neurons or regular spiking neurons (33% and 50%, respectively, Table 2). Burst spiking neurons are strongly activated in all-or-none fashion at their firing threshold, showing transient burst firing. These properties may enable these neurons to respond sensitively to changes in synaptic inputs, and may be well suited for the detection of changes in visual events. The burst firing occurred only when the neuron was excited at more hyperpolarized level. Such voltage dependency suggests that response of burst spiking neurons are affected by balance of tonic excitatory and inhibitory inputs.

In addition to burst spiking neurons which showed transient burst firing, regular spiking neurons also showed higher frequency of firing in the beginning of the depolarizing current pulses, compared with its later part due to the spike frequency adaptation. Most of regular spiking neurons recorded in the present study showed moderate spike frequency adaptation. Furthermore, neurons with short spike train and neurons with rapid spike inactivation also showed transient firing. Thus, vast majority of neurons recorded in this study can show transient high frequency firing to excitatory input. Previous studies have indicated that the majority of neurons in the superficial layer of the SC shows phasic response to visual stimulation and well respond to moving stimuli (e.g., Cynader and Berman, 1972; Goldberg and Wurtz, 1972a; Humphrey, 1968; Schiller and Koener, 1971). These visual response properties of neurons in the superficial layer may at least partly depend on transient nature of firing properties of the neurons.

The present study provides evidence for the presence of specific ionic conductances in SC superficial layer neurons. Inward rectification appears to be due either to IRK channels or I_h channels. Lo et al. (1998) demonstrated that Ca^{2+}-activated K^+ channels play a significant role in detemining the firing frequency of SO neurons. Although not specifically

investigated in this study, the channels may also contribute to spike frequency adaptation in regular spiking neurons recorded in the present study. These channels are known to be significantly modulated by several neurotransmitter systems (see Nicoll et al., 1990). Such modulatory actions should contribute to modulation of activity of SC superficial layer neurons by levels of arousal and attention.

		Burst	Regular	Late	Fast	Short train	Inactivation
number of neurons	total	87	131	20	9	11	4
	with time-dependent inward redification	45	61	7	4	1	2
	with time-independent inward redification	24	31	4	3	4	0
input resistance (MΩ)		578±47 (3067~121)	712±36 (2054~82)	819±90 (1425~244)	878±151 (1711~274)	888±104 (1396~329)	835±271 (1494~239)
capacitance (pF)		24±1 (58~6)	23±1 (80~4)	18±2 (43~8)	12±3 (29~4)	17±3 (34~5)	11±1 (14~9)

Table I-1.

Electrophydiological properties of neurons in the superficial layer of the rat SC
Values are expressed as mean ± S.E.M and range (in parentheses)

			Marginal	NFV	Piriform	Horizontal	Stellate	WFM	WFV
number of recorded neurons	total		6	15	14	18	9	8	28
	Burst spiking	total	0	5	8	3	5	1	13
		with time-dependent inward rectification	0	2	6	3	0	0	13
		with time-independent inward rectification	0	1	1	0	2	1	0
	Regular spiking	total	4	9	3	14	3	5	15
		with time-dependent inward rectification	1	4	1	9	1	1	15
		with time-independent inward rectification	3	2	0	1	2	3	0
	Other types		1 Short 1 Short / TIIR	1 Late	1 Late / TDIR 1 Short 1 Short / TDIR	1 Inadivation	0	1 Late 1 Fast / TIIR	0
	input resistance (MΩ)		604±48 (839±507)	562±74 (1082~197)	760±114 (1765~184)	727±77 (1494~343)	843±149 (1859~491)	680±111 (1157~305)	148±8 (264~82)
	capacitance (pF)		27±4 (35~9)	23±5 (80~11)	19±3 (43~8)	19±2 (39~10)	26±5 (53~9)	21±4 (45~7)	34±2 (54~8)

Table I-2.

Electrophysiological properties and morphological characteristics. Values are expressed mean ± S.E.M. and range (in parentheses). NFV: narrow field vertical cells. WFM: wide field multipolar cells. WFV: wide field vertical cells.

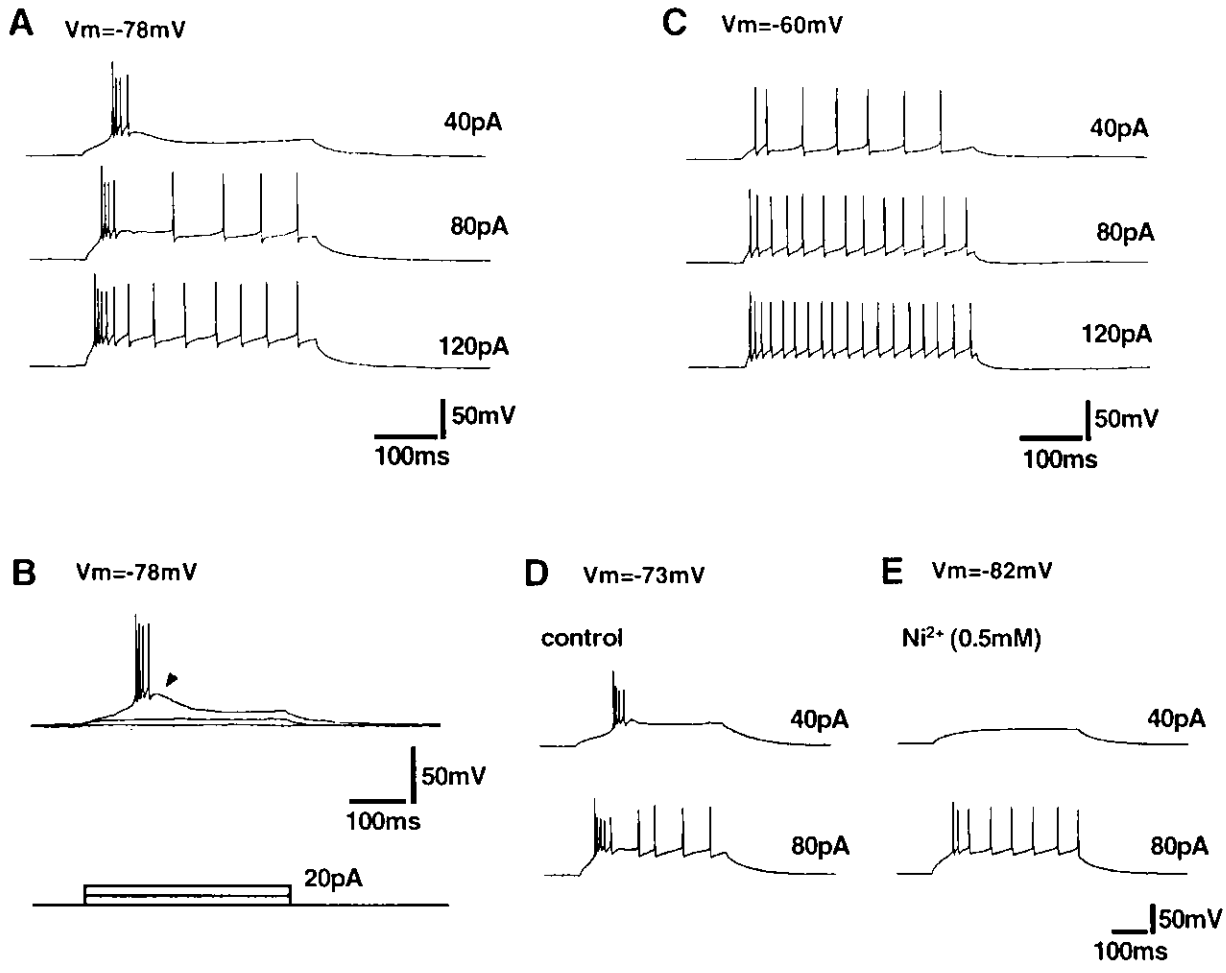

Figure I-1. Electrophysiological properties of burst spiking neurons.

A–C are recordings from same neuron. D and E are from another neuron. A and B: responses to depolarizing current pulses from hyperpolarized membrane potential (-78mV). A: responses to depolarizing current pulses (values given at right). B, *top*: responses to current pulses near threshold for spike generation. *Bottom*: Injected current pulses. C: responses to depolarizing current pulses (values given at right) from depolarized membrane potential (-60mV). D and E: effect of Ni^{2+} on transient burst. Control (D) and during application of 0.5mM Ni^{2+} (E). Values of injected current pulses were given at right.

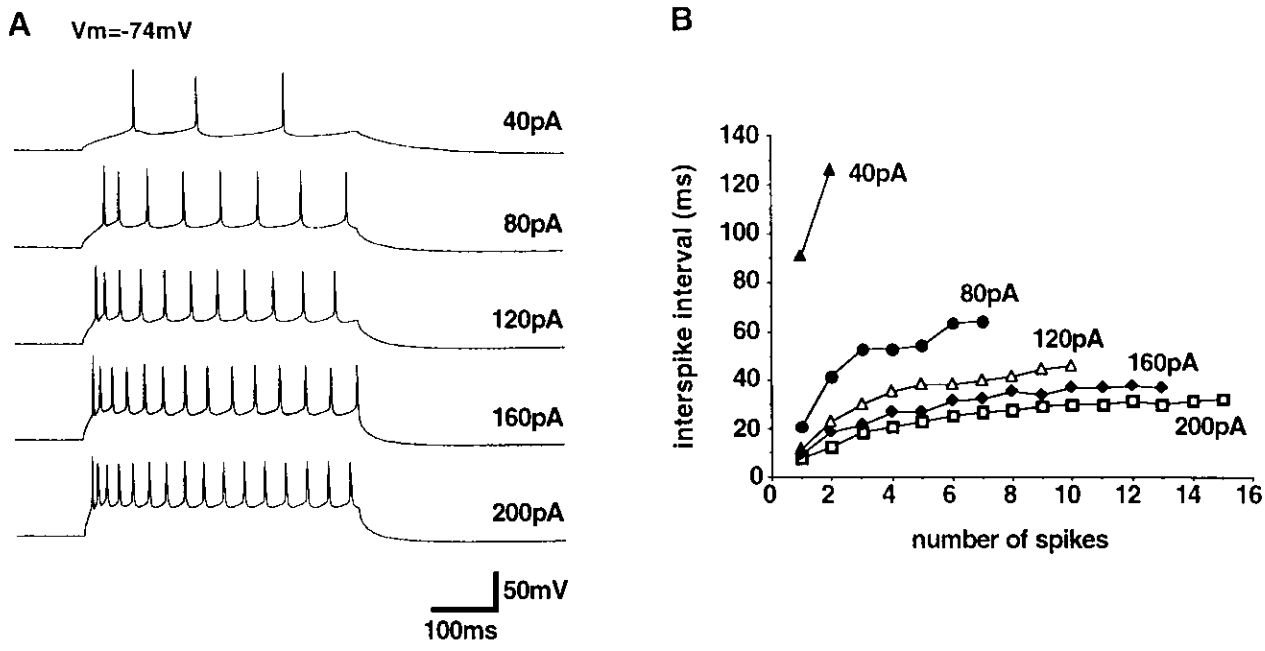

Figure I-2. Electrophysiological properties of a regular spiking neuron

A: responses to depolarizing current pulses (values given at right). B: interspike interval between successive spikes, recorded at different current intensities.

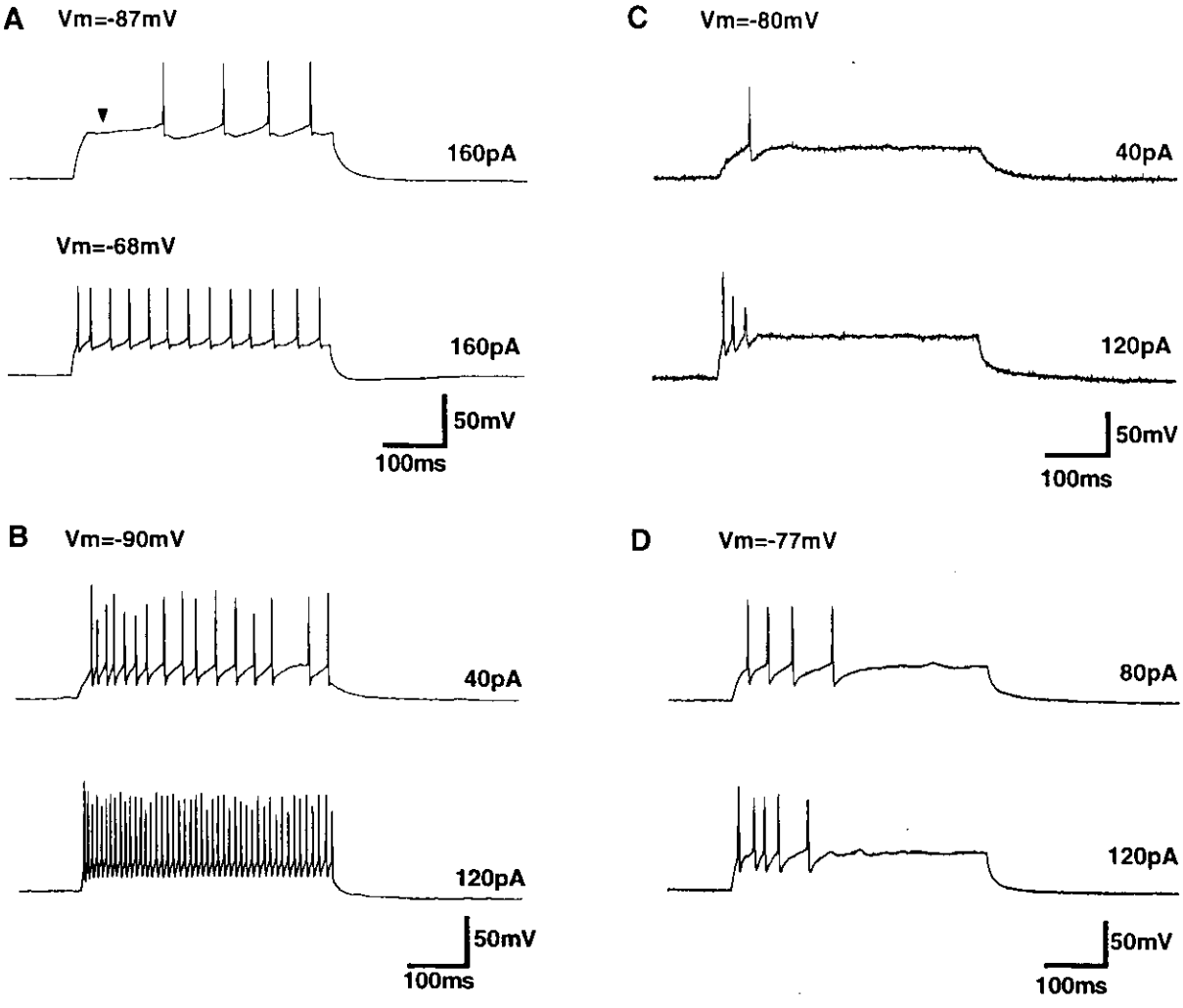

Figure I-3. Electrophysiological properties of neurons in four minor populations.

A: responses to depolarizing current pulses (values given at right) of a late spiking neuron. The current pulses were injected from two different membrane potentials (-87mV, *top*; -68mV, *bottom*). B–D: responses to depolarizing current pulses (values given at right) of a fast spiking neuron (B), a neuron with rapid spike inactivation (C) and a neuron with short spike train (D).

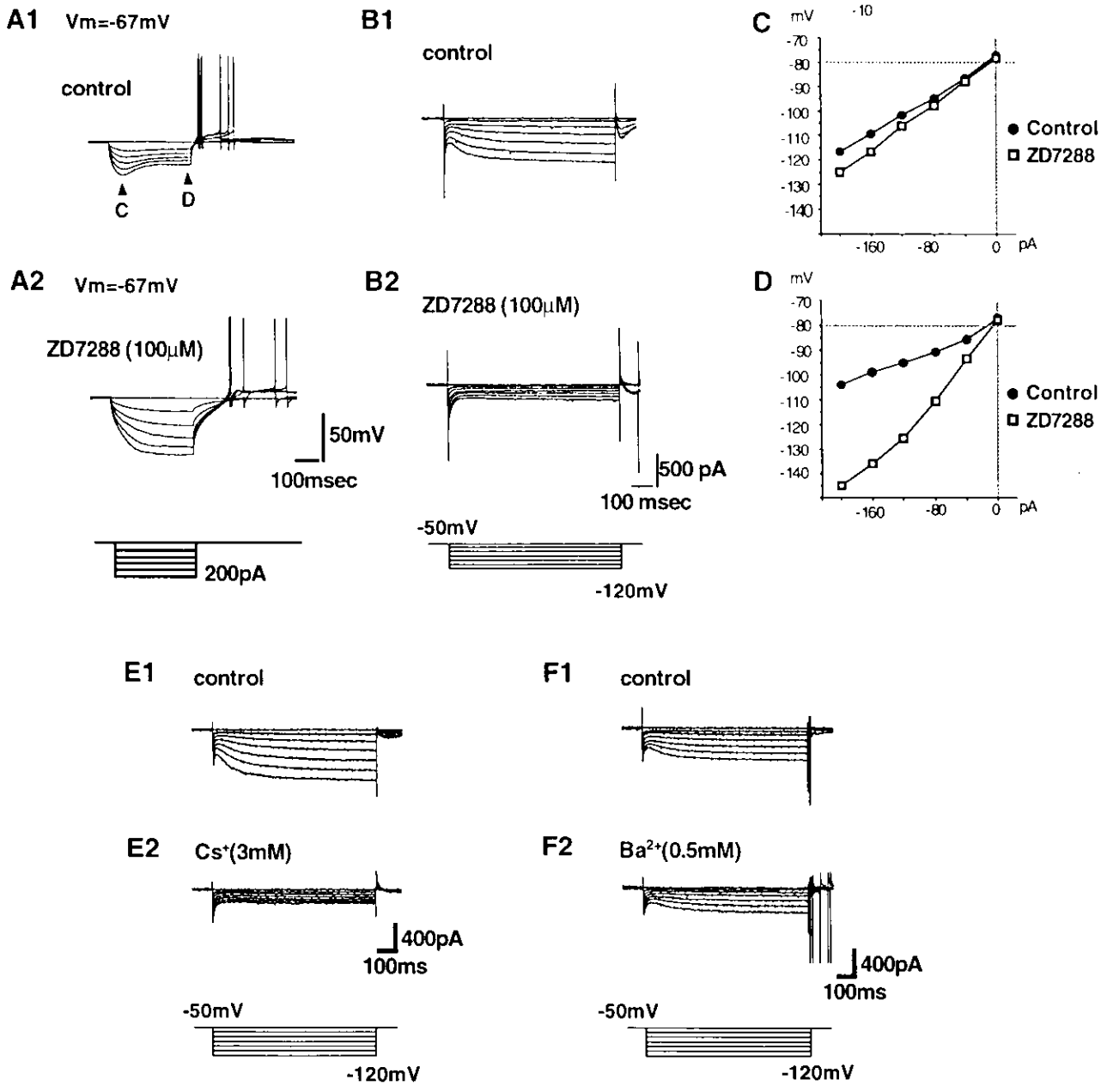

Figure I-4. Time-dependent inward rectification.

A: responses to hyperpolarizing current pulses in the control solution (A1) and during application of 100μM ZD7288 (A2, *top*). Injected current pulses are shown at *bottom* of A2. B: voltage clamp recordings from same neuron shown in A. Responses to hyperpolarizing voltage steps from -60mV in the control solution (B1) and during application of 100μM ZD7288 (B2, *top*). Applied voltage steps are shown at *bottom* of B2. C and D: current-voltage plots for traces shown in A. The membrane potential at peak (C; 55 to 75msec from onset of current pulse) and steady-state level (D; 375 to 395msec from onset of current pulse). E: effect of Cs^+ on time-dependent inward rectifier currents. Control (E1) and during application of 3mM Cs^+ (E2). Applied voltage steps are shown at bottom of E2. F: effect of Ba^{2+} on time-dependent inward rectifier currents. Control (F1) and during application of 0.5mM Ba^{2+} (F2). Applied voltage steps are shown at bottom of F2.

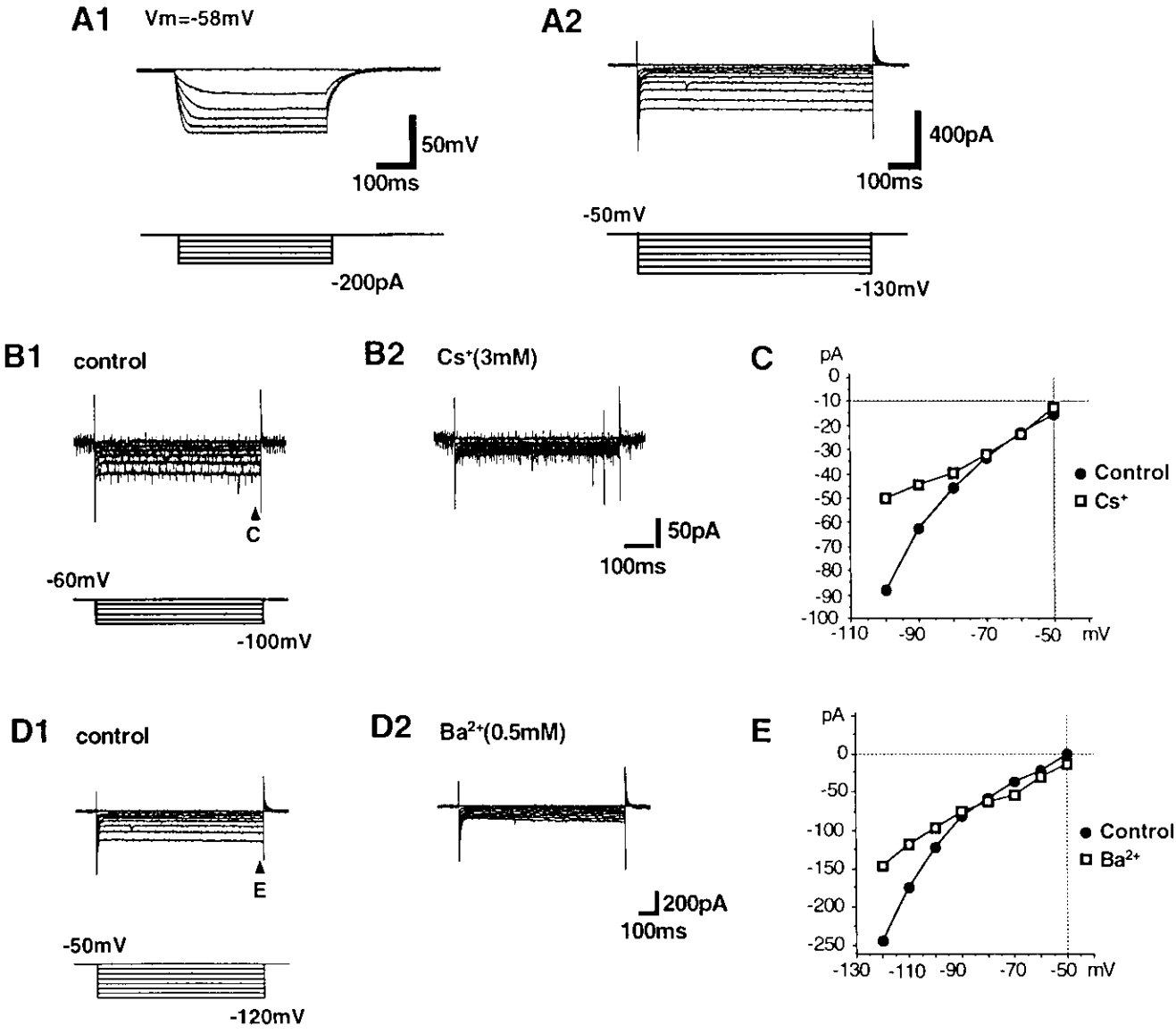

Figure I-5. Time-independent inward rectification.

A: current clamp recordings (A1, *top*) and voltage clamp recordings (A2, *top*) from same neuron. Applied current and voltage steps are shown at *bottom*. B and C: effect of Cs^+ on time-independent inward rectifier currents. B: voltage clamp recordings in the control solution (B1, *top*) and during application of 3mM Cs^+ (B2). Applied voltage steps are shown at *bottom*. C: current-voltage plots for traces shown in B. The current values at stedy-state level (775 to 795 msec from onset of the voltage step) were measured and plotted. D and E. effect of 0.5mM Ba^{2+} on time-independent inward rectifier currents. Details as in B and C.

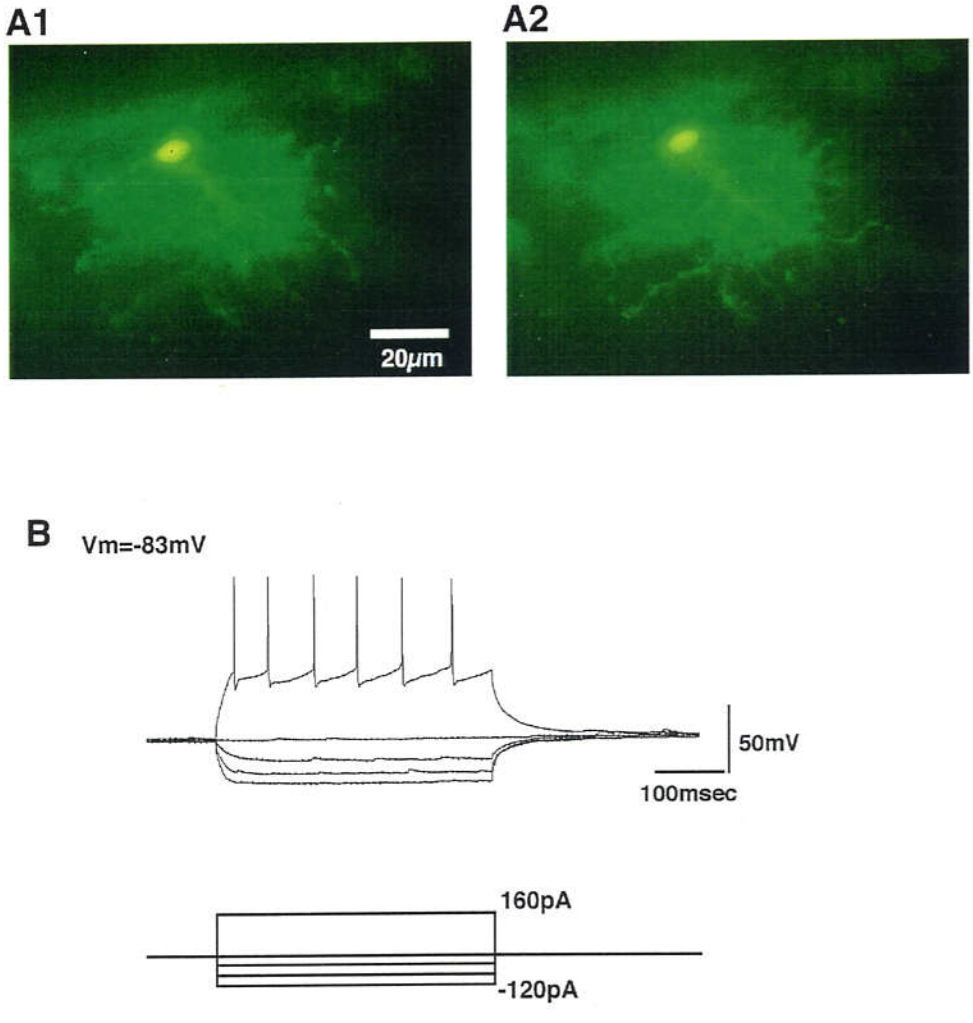

Figure I-6. A marginal cell

A1 and A2: photomicrographs of a lucifer yellow-filled marginal cell taken at different focal plane. B: responses of the cell in A to current pulses (top) and injected current pulses (bottom).

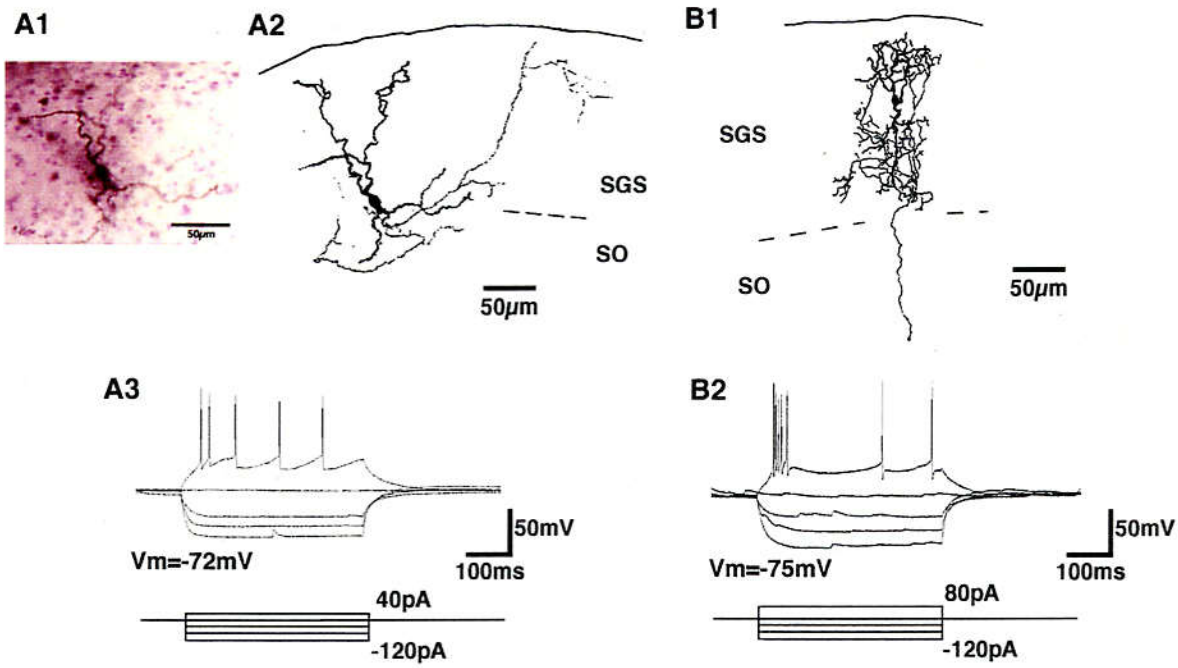

Figure I-7. Narrow field vertical cells

A1: photomicrograph of a narrow field vertical cell stained with biocytin. A2: camera lucida drawing of the cell in A1. The axon is drawn in thin line. A3: responses of the cell in A1 and A2 to current pulses (top) and injected current pulses (bottom). B: another narrow field vertical cell. Camera lucida drawing (B1) and responses to current pulses (B2). Details as in A.

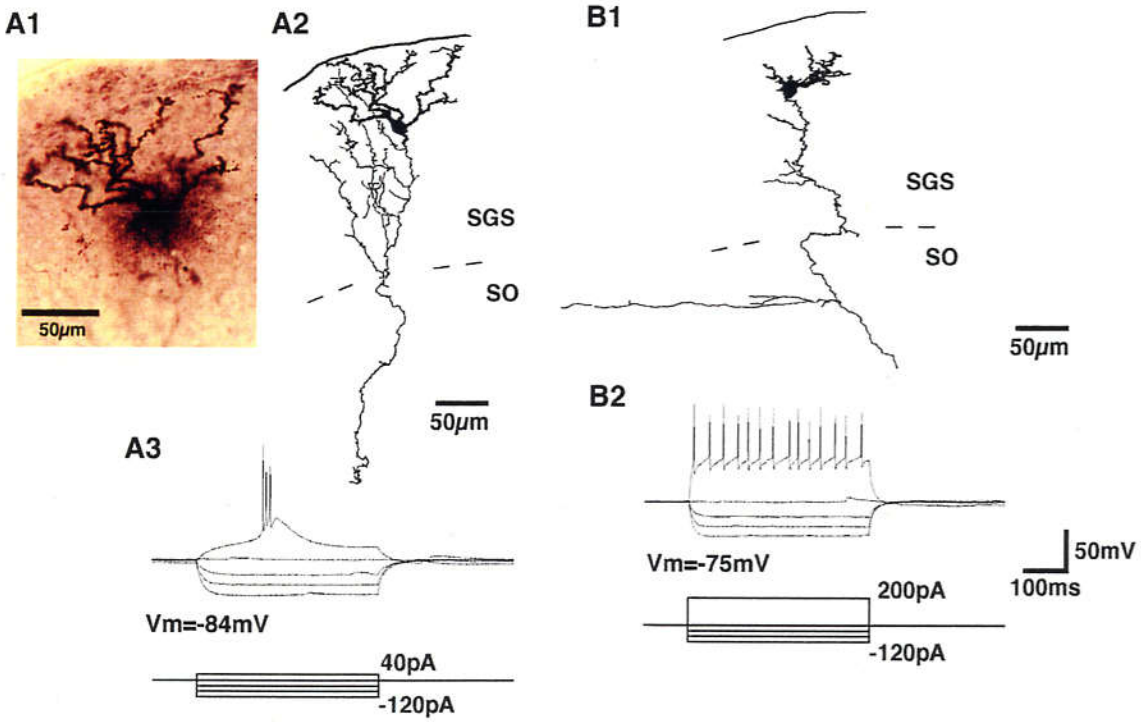

Figure I-8. Piriform cells.

A1: photomicrograph of a piriform cell stained with biocytin. A2: camera lucida drawing of the cell in A1. The axon is drawn in thin line. A3: responses of the cell in A1 and A2 to current pulses (top) and injected current pulses (bottom). B: another piriform cell. Camera lucida drawing (B1) and responses to current pulses (B2). Details as in A.

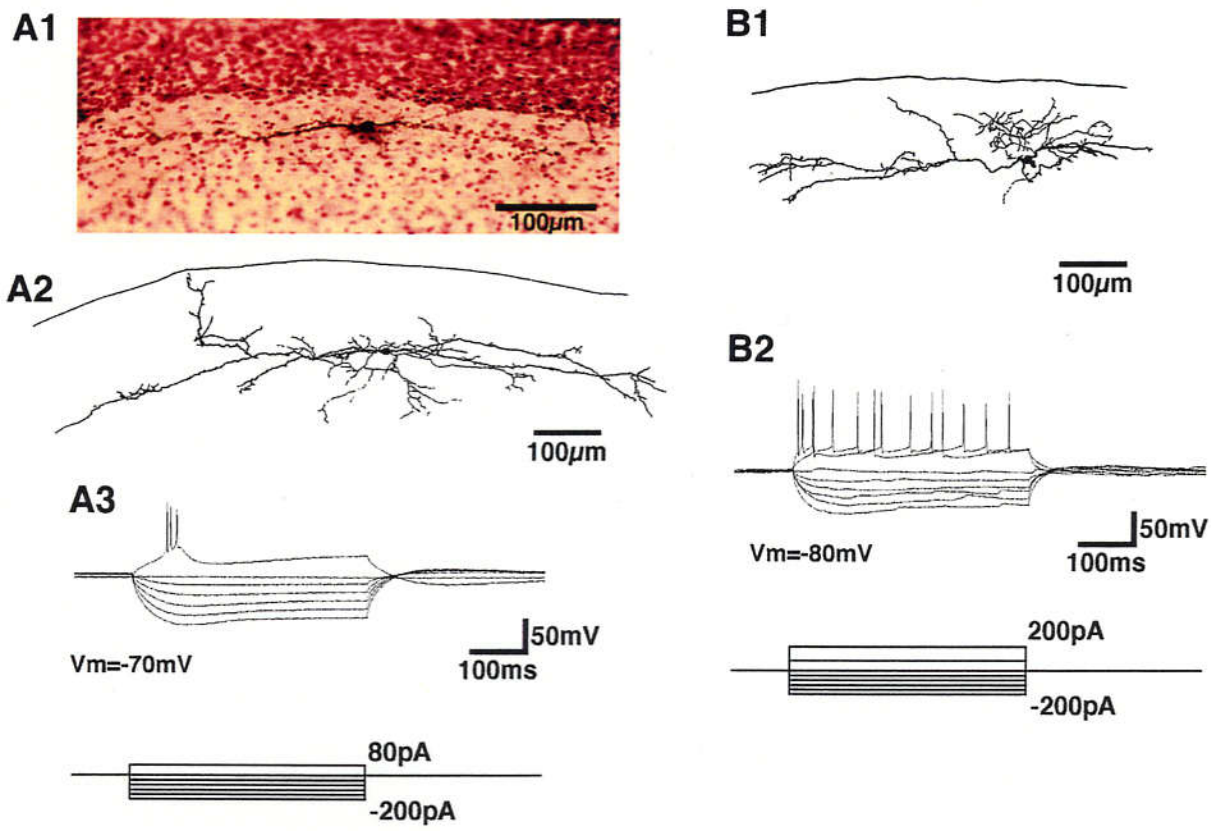

Figure I-9. Horizontal cells.

A1: photomicrograph of a horizontal cell stained with biocytin. A2: camera lucida drawing of the cell in A1. The axon is drawn in thin line. A3: responses of the cell in A1 and A2 to current pulses (top), and injected current pulses (bottom). B: another horizontal cell. Camera lucida drawing (B1) and responses to current pulses (B2). Details as in A.

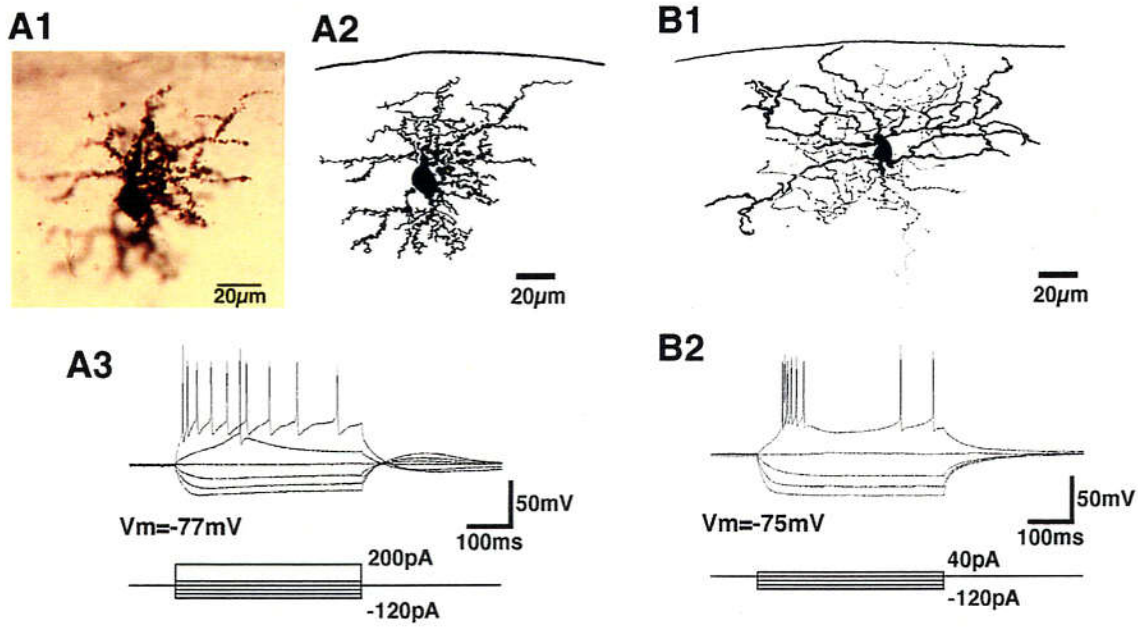

Figure I-10. Stellate cells.

A1: photomicrograph of a stellate cell stained with biocytin. A2: camera lucida drawing of the cell in A1. The axon could not be traced. A3: responses of the cell in A1 and A2 to current pulses (top) and injected current pulses (bottom). B: another stellate cell. Camera lucida drawing (B1), responses to current pulses (B2, top) and injected current pulses (bottom). The axon is drawn in thin line.

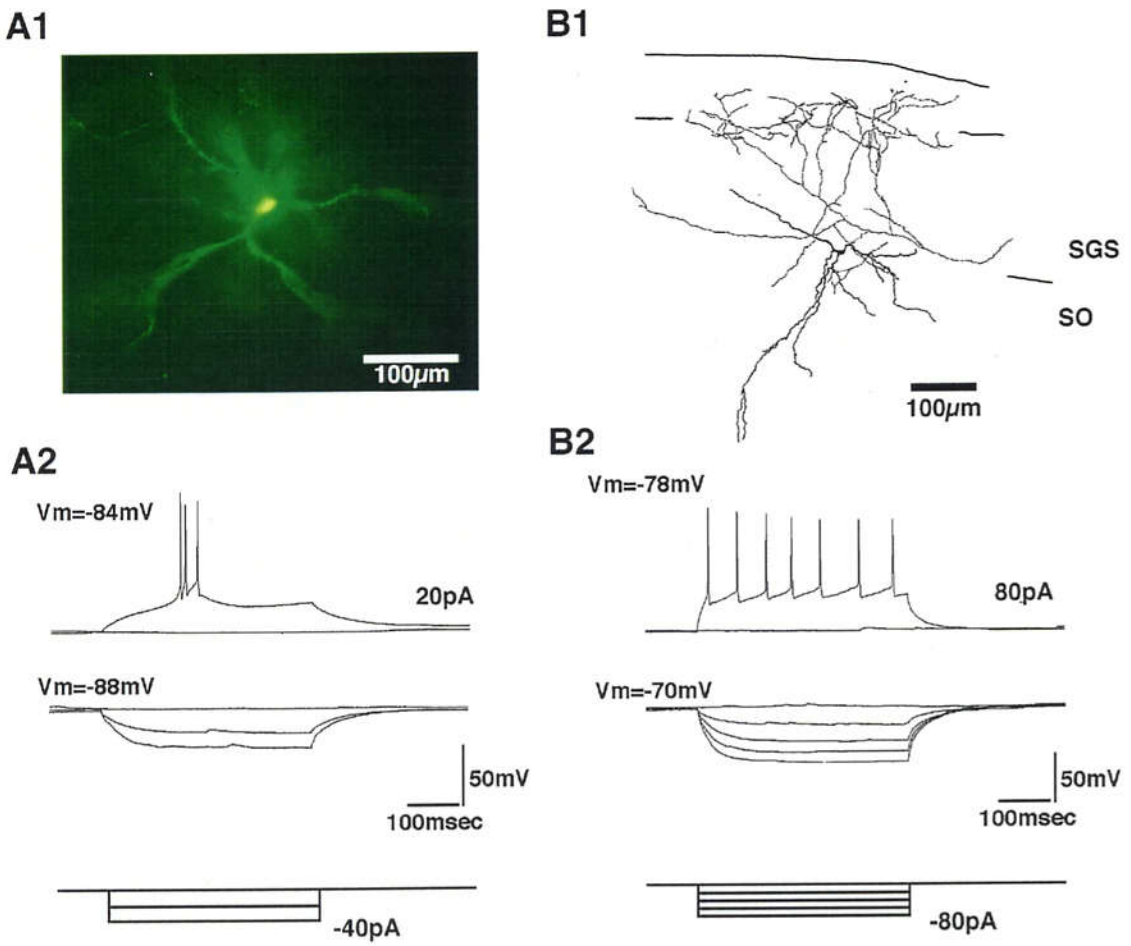

Figure I-11. Wide field multipolar cells.

A1: photomicrograph of a wide field multipolar cell stained with lucifer yellow. A2: responses of the cell in A1 to current pulses. B: another wide field multipolar cell. Camera lucida drawing (B1), responses to current pulses (B2). The axon is drawn in thin line.

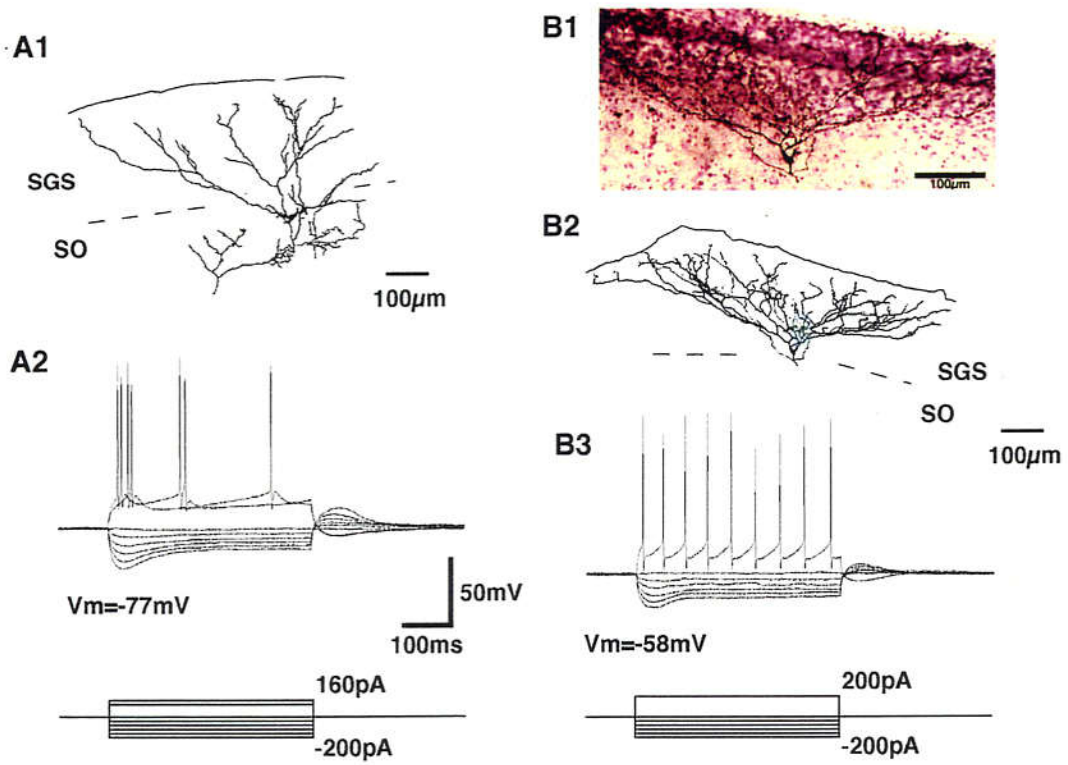

Figure I-12. Wide field vertical cells.

A: another stellate cell. Camera lucida drawing (A1), responses to current pulses (A2, top) and injected current pulses (bottom). The axon is drawn in thin line. B1: photomicrograph of a stellate cell stained with biocytin. B2: camera lucida drawing of the cell in B1. The axon is drawn in thin line. B3: responses of the cell in B1 and B2 to current pulses (top) and injected current pulses (bottom).

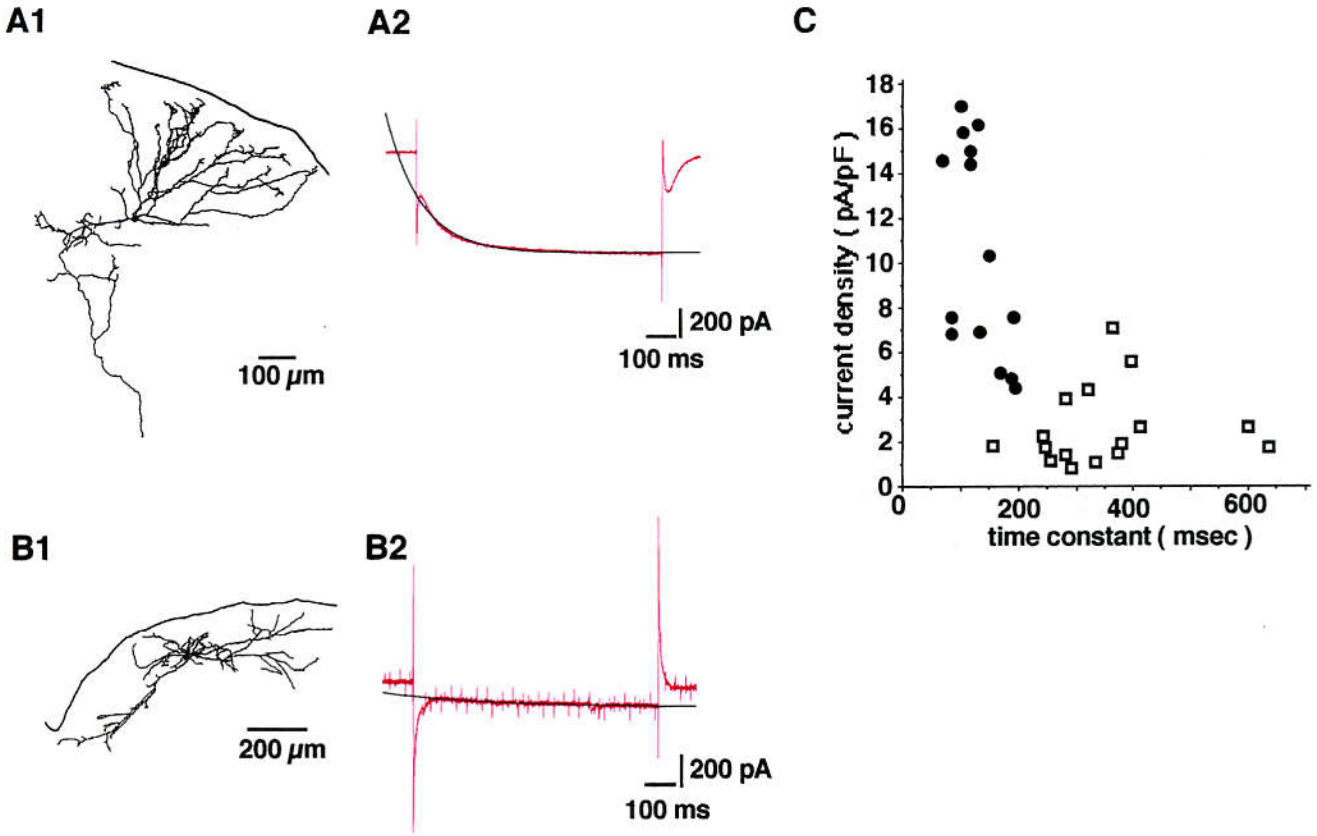

Figure I-13. Activation kinetics of I_h in wide field vertical cells and other cells.

A1: camera lucida drawing of a wide field vertical cell. A2: a current response (red trace) of the wide field vertical cell shown in A1 to a voltage step from -50mV to -100mV was fitted with a single exponential function (black line). The time constant and the steady-state current density of the I_h were 117msec and 14.4pA/pF, respectively. B1: camera lucida drawing of a horizontal cell. B2: a current response (red trace) of the horizontal cell shown in B1 to a voltage step from -60mV to -110mV was fitted with a single exponential function (black line). The time constant and the steady-state current density of the I_h were 378msec and 1.95pA/pF, respectively. C: plot of steady-state current density against time constant. Data from wide field vertical cells (filled circles) and from other cells (open squares).

Chapter II

Organization of Excitatory Synapses; Distribution of Functionally Different Subtypes of AMPA-type Glutamate Receptors in Morphologically Different Cell Subtypes

Summary

Rectification property and Ca^{2+}-permeability of AMPA-type glutamate receptors were investigated in seven morphologically identified subclasses of neurons in the superficial layer of the superior colliculus by whole-cell patch clamp recording technique in slice preparations obtained from rats (PND17-23). Among these subclasses of neurons, AMPA receptors with inwardly rectifying current-voltage (I-V) relationship were found mainly in horizontal cells, while linear or outwardly rectifying AMPA receptors were found in all the seven cell types. The inwardly rectifying AMPA receptors were suppressed by 1 mM spermine, while those with linear or outwardly rectifying I-V relationship were not. The degree of inward rectification was inversely correlated with the reversal potential of current responses of AMPA receptors in Na+-free, isotonic high Ca^{2+} (20mM) solution, which is an indicator of Ca^{2}+-permeability of the receptors. Thus, Ca^{2}+-permeability was higher in inwardly rectifying AMPA receptors. Furthermore, the AMPA-component of excitatory post-synaptic currents which showed inwardly rectifying I-V relationship and markedly suppressed by 1mM spermine was evoked by electrical stimulation. These results indicate that Ca^{2+}-permeable AMPA receptors are mainly expressed in horizontal cells and involved in synaptic transmission.

Introduction

We have investigated the membrane properties of morphologically identified neurons in the SC superficial layer in chapter I. To understand the mechanisms of information processing in the local circuits, it is also essential to obtain the information about synaptic mechanisms of these neurons.

Glutamate is a major excitatory neurotransmitter in the central nervous system, and -amino-3-hydroxy-5-methyl-4-isoxazolepropionic acid (AMPA)-type glutamate receptor channels mediate fast excitatory synaptic transmission. AMPA receptors have been classified into two functionally distinct subtypes (Iino et al., 1990; Ozawa and Iino., 1993). One of them (type I) exhibits an outwardly rectifying current-voltage (I-V) relationship and little Ca^{2+} permeability, and the other receptor subtype (type II) show inwardly rectifying I-V relationship and high Ca^{2+} permeability. Molecular biological studies clarified that the former receptors include GluR2 subunit, while the latter lack the GluR2 subunit (Hollmann et al., 1991; Geiger et al., 1995; Jonas and Burnashev, 1995). Type II AMPA receptors are expressed in various neuronal cell types in the central nervous system such as hippocampal interneurons, basket cells in the hippocampus, neocortical interneurons, spinal dorsal horn neurons (Bochet et al., 1994; Gu et al., 1996; Isa et al., 1996; Itazawa et al., 1997; Mcbain and Dingledine, 1993). Recently, several investigations have demonstrated functional significance of Ca^{2+} influx through type II AMPA receptors. Type II AMPA receptors mediate enhancement of amplitude of miniature EPSCs (Gu et al., 1996), long-term potentiation (Mahanty and Sah, 1998) and long-term depression (Laezza et al., 1999). Furthermore, type II AMPA receptors modulate glycine-evoked Cl^- currents (Xu et al., 1999) and suppress NMDA receptor-

mediated currents (Kyrozis et al. 1995).

In this study, we investigated the subtype of AMPA receptors expressed in individual morphologically identified SC superficial layer neurons. The results suggest that all subclasses of neurons express type I AMPA receptors and type II AMPA receptors were additionally expressed mainly in horizontal cells.

Methods

The methods employed in this study were in general similar to those described in chapter I of this thesis. Frontal slices (300μm thick) of the SC were prepared from 16- to 23-day-old Wistar rats following ether anesthesia. The slices were incubated at room temperature for > 1 hour in control Ringer's solution before recording. Whole-cell patch clamp recordings (Edwards et al. 1989; Hamill et al. 1981) were obtained from neurons using visual control of the patch pipettes. The control Ringer's solution contained (mM) : 125 NaCl, 2.5 KCl, 2 $CaCl_2$, 1 $MgCl_2$, 26 $NaHCO_3$, 1.25 NaH_2PO_4, 25 glucose, and continuously bubbled with 95 % O_2 and 5 % CO_2 (pH 7.4). Intracellular solution contained (mM) : 120 Cs-gluconate, 20 CsCl, 10 EGTA, 2 $MgCl_2$, 2 Na_2ATP, 10 HEPES, 0.1 spermine, 5 Qx-314, pH 7.3. To investigate the current responses mediatd by AMPA receptors, kainic acid was used as non-desensitizing agonist of AMPA receptors. Kainic acid was applied to the recorded cells either by air pressure (10 mM kainic acid was dissolved in the standard Ringer's solution and applied with 5 - 20 psi, 5 – 20 ms square pulse generated by PV920, World Precision Instruments, Sarasota, FL) or bath application (100 μM kainic acid was used). Since kainate receptors are supposed to be desensitized under this condition, the current responses obtained in the present study was attributed to activation of AMPA receptors. To obtain the current-voltage (I-V) relationship of the kainate responses, holding potentials were systematically changed in case of air pressure application. In the case of bath application, the membrane potential was ramped from –60 or –70 to +60 mV and then shifted down from +60 to –60 or –70mV again at a rate of 50mV/s. The current records in the latter phase were used. The I-V curve was obtained by subtracting the current recorded in the standard Ringer's solution from that obtained in the presence of

kainate. To estimate Ca^{2+}-permeability, the reversal potential of KA-induced currents in the isotonic Na^+-free, isotonic high Ca^{2+} solution was measured. In this experiment, the control solution contained (mM): 145 NaCl, 2.5 KCl, 2 $CaCl_2$, 1 $MgCl_2$, 5 HEPES, 10 glucose, was bubbled with 100% O_2 (pH 7.4). The Na^+-free, isotonic high Ca^{2+} solution contained (mM): 20 $CaCl_2$, 10 glucose, 5 HEPES, 144 N-methyl-glucamine (NMG), and was bubbled with 100% O_2 (pH 7.4). When kainate-responses were investigated in the Na^+-free, isotonic high Ca^{2+} solution, kainic acid was applied to the recorded cells by air pressure (10 mM kainic acid was dissolved in the Na^+-free, isotonic high Ca^{2+} solution). Excitatory postsynaptic currents (EPSCs) were evoked by electrical stimulation (cathodal square wave current pulses, 33–42 μA, 0.2 ms duration) with a glass pipette containing 2M NaCl solution placed about 100μm away from the recorded neuron. To stain the recorded neurons, biocytin (5mg/ml, Sigma, St. Louis, MO) was dissolved in the solution. After recording, slices were fixed with 4% paraformaldehyde and recorded neurons were visualized by staining with biocytin (Horikawa and Armstrong, 1988), using ABC method. Kainic acid was obtained from Sigma. Tetrodotoxin (TTX) was from Sankyo (Tokyo, Japan). TTX was bath applied.

Results

Rectification properties of kainate (KA)-responses

I-V relationship of responses to kainic acid (KA) was investigated in 125 neurons in the SC superficial layer either by pressure application or bah application. As shown in previous studies on the rectification properties of AMPA receptors (Iino et al., 1990; Isa et al., 1996; Itazawa et al., 1997), both KA response with linear or outward rectification and that with inward rectification could be observed. Rectification properties were estimated as rectification index (RI) with following equation,

$RI = -(I_{Erev+40} / 40) / (I_{Erev-60} / 60)$

where $I_{Erev+40}$ and $I_{Erev-60}$ were the amplitudes of the KA-induced currents at the reversal potential (E_{rev}) plus 40 mV and the E_{rev} minus 60 mV, respectively. According to this index, inward rectification is expressed as RI <1.0, whereas outward rectification as RI > 1.0. KA-responses with R.I. > 1.0 were classified as Type I responses, those with R.I. < 0.25 were classified as Type II responses and those with $0.25 \leqq$ R.I. $\leqq 1.0$ were classified as intermediate type responses (Iino et al., 1994).

Figure II-1 exemplifies the current response which showed slight outward rectification . Fig. II-1A and B shows the current responses to pressure application of 10mM KA at different membrane potentials and its current-voltage (I-V) relationship, respectively. The rectification index in this case was 1.17. This type of KA-response has been described as type I response (Ozawa et al. 1991, Iino et al., 1994). The effect of 1 mM spermine, a specific antagonist of type II AMPA receptors (Isa et al. 1996), was tested on the KA-induced currents in 3 neurons in the SC superficial layer with type I response and it was turned out to be ineffective in all the cases as shown in Fig. 1C.

Figure II-2 shows another type of KA responses. In this neuron, its I-V relationship showed inward rectification between –80 and +40 mV. Above +40 mV, the I-V relationship showed outward rectification. The rectification index was 0.44. This type of KA-response has been classified as "intermediate type" according to Iino et al., (1994). Application of 1 mM spermine showed reduction in the KA-induced current by 43 %. The effect of 1 mM spermine was tested in 3 neurons in the SC superficial layer neurons with inwardly rectifying KA-responses and suppression of 17 – 43 % in amplitude could be observed.

Ca^{2+}-permeability of KA-responses and its relationship to the rectification propert y

As a following step, Ca2+-permeability was examined by measuring the reversal potential of KA-induced currents in the isotonic Na^+-free, isotonic high Ca^{2+} solution (20mM Ca^{2+}). Figure II-3 shows an example of neurons with type I KA-response (RI=1.15). In this case, the reversal potential of the KA response in the Na-free, isotonic high Ca^{2+} solution was –92mV. P_{Ca}/P_{Cs} value estimated from the reversal potential using the constant-field equation (Iino et al. 1990) was 0.05, which indicates low permeability to Ca^{2+}. In contrast, in the neuron shown in Fig. II-4, that showed intermediate-type KA-response (RI=0.38), the reversal potential in the Na^+-free, isotonic high Ca^{2+} solution was –23mV and the estimated value of P_{Ca}/P_{Cs} was 1.04, which indicated relatively high Ca^{2+}-permeability.

Figure II-5 indicates the relationship between the reversal potential of the KA-response in the Na^+-free, isotonic high Ca^{2+} solution and RI in twelve neurons in the SC superficial layer. As shown in the figure, there was a clear negative correlation between the RI and the reversal potential in the Na^+-free, isotonic high Ca^{2+} solution, which was a measure of Ca^{2+}

permeability, as has been shown in hippocampal and neocortical neurons (Isa et al. 1996; Itazawa et al. 1997). The observation that the values of RI were distributed over a wide range suggest that the neurons in the SC superficial layer express both Type I and Type II AMPA receptors with a varying ratio from cell to cell.

Expression of different AMPA receptor subtypes in the morphologically identified cell subclasses

We investigated the RI values of the KA-responses in 70 morphologically identified cells. These cells consisted of 29 horizontal cells, 12 stellate cells, 6 narrow field vertical cells, 7 piriform cells, 7 wide field vertical cells, 5 marginal cells and 4 wide field multipolar cells. Morphological characteristics of these subclasses were described in chapter I. Figure II-6A shown an example of a stellate cell with outwardly rectifying KA-response (RI=1.41). Figure II-6B shows an example of stained horizontal cell and its KA-response with inward rectification (RI=0.72). Figure II-7 shows the distribution of RI values of KA-responses in all the 70 morphologically identified neurons in the SC superficial layer. As shown in the figure, only horizontal cells included substantial number of neurons with inwardly rectifying KA-responses. The neurons with inwardly rectifying KA-responses consisted of 59 % (17 / 29) of the horizontal cells tested. This result suggests that type II AMPA receptors were mainly expressed in horizontal cells in the superficial layer of the SC.

Inwardly rectifying and spermine-sensitive EPSCs

The results described above suggest that the inwardly rectifying and Ca^{2+}-permeable AMPA receptors are expressed in a population of neurons in the superficial layer of the rat SC. We next investigated that these receptors

are involved in synaptic transmissions onto neurons in the SC superficial layer. Figure II-8A and B shows an example of EPSCs evoked by electrical stimulation near the recorded cell and the I-V relationship of the peak amplitude of the EPSCs, respectively. The recording were obtained under the presence of 50 μM APV. The RI value was 0.75. The EPSCs were suppressed by 1 mM spermine (Fig. II-8C) by 32 %. Thus, we could recorded EPSCs which had inwardly rectifying I-V relationship and were suppressed by spermine (n=2), suggesting that inwardly rectifying and Ca^{2+} permeable AMPA receptors are involved in synaptic transmissions onto neurons in the SC superficial layer.

Discussion

The results of present study have shown that both neurons with linear or outwardly rectifying I-V relationship of AMPA receptor-mediated current and those with inwardly rectifying I-V relationship of AMPA receptor-mediated current are present in the superficial layer of the SC. E_{rev} in Na^+-free, isotonic high Ca^{2+} solution is inversely correlated with RI value, indicating that neurons with stronger inward rectification showed higher Ca^{2+}-permeability. Previous studies have demonstrated that two types of functionally different AMPA receptors are expressed in cultured hippocampal neurons: one mediates outwardly rectifying KA- or AMPA-responses and displays little Ca^{2+}-permeability (type I response caused by Type I AMPA receptors), the other mediates inwardly rectifying KA- or AMPA-responses and displays a substantial Ca^{2+}-permeability (type II response caused by Type II AMPA receptors; Iino et al., 1990; Ozawa and Iino, 1993). The present study also showed that inwardly rectifying KA-responses are suppressed by 1mM spermine, consisting with known properties of Type II AMPA receptors (Isa et al., 1996). Taken together, the results of present study suggest that both outwardly rectifying, Ca^{2+}-inpermeable Type I AMPA receptors and inwardly rectifying, Ca^{2+}-permeable Type II AMPA receptors are expressed in neurons in the superficial layer of the rat SC. Since RI values and E_{rev} in Na^+-free, isotonic high Ca^{2+} solution are scattered throughout the range rather than concentrated in two regions of extreme values, each neuron in the superficial layer of the rat SC may expresses two types of AMPA receptors with various relative amount (Bochet et al., 1994; Geiger et al., 1995; Jonas et al., 1994). Furthermore, we could recorded EPSCs which had inwardly rectifying I-V relationship and were suppressed by spermine, suggesting that inwardly rectifying and Ca^{2+} permeable AMPA

receptors are involved in synaptic transmissions onto neurons in the SC superficial layer.

A number of studies have described several types of morphologically different neurons in the superficial layer of the rat SC (Langer and Lund, 1974; Tokunaga and Otani, 1976; Labriola and Laemle, 1977; Endo, in chapter I of this thesis). The results of the present study suggest that Type I AMPA receptors are expressed in all types of neurons, in contrast, Type II AMPA receptors are mainly expressed in a type of neurons, horizontal cells. Most brain neurons which were reported to express the Type II AMPA receptors are GABAergic and express a Ca^{2+} binding protein, parvalbumin (Bochet et al., 1994; Jonas et al., 1994; Kondo et al., 1997; Leranth et al., 1996). Horizontal cells in the superficial layer of the SC are also supposed to be GABAergic (Mize, 1992). However, very few of the parvalbumin immunoreactive cells are GABAergic in the SC (Mize, 1992). In addition, although parvalbumin immunoreactive horizontal cells were observed (Cork et al., 1998), these cells appear not to be major population among parvalbumin immunoreactive cells in the superficial layer of the rat SC (e.g., Cork et al., 1998; Illing et al., 1990). Thus, it may be necessary to consider another rule with respect to colocalization of the type II AMPA receptors and parvalbumin in the superficial layer of the rat SC.

Functional significance of the expression of the Ca^{2+}-permeable AMPA receptors in horizontal cells are presently unclear. Horizontal cells in the superficial layer of the SC are thought to mediate surround inhibition based on their horizontally long morphology. Recently, Ca^{2+} influx through Ca^{2+}-permeable AMPA receptors have been suggested to mediate several types of modulatory functions, such as enhancement of amplitude of miniature EPSCs (Gu et al., 1996), long-term potentiation (Mahanty and Sah, 1998), long-term depression (Laezza et al., 1999), enhancement of glycine-

evoked Cl^- currents (Xu et al., 1999) and suppression of NMDA receptor-mediated currents (Kyrozis et al. 1995). If Ca^{2+}-permeable AMPA receptors in horizontal cells mediate regulation of strength of synaptic transmission onto these cells, the effects may modulate the receptive field properties of neurons in the superficial layer of the SC.

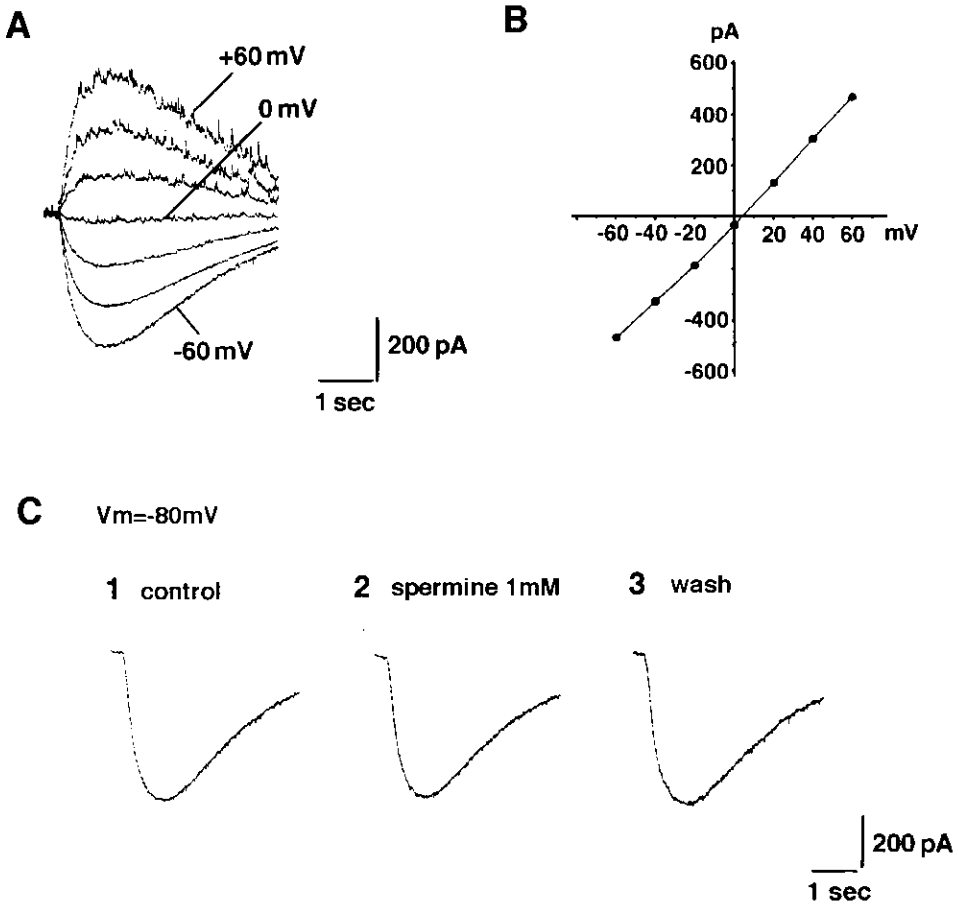

Figure II-1. Outwardly rectifying KA-response.

A: current responses to pressure applied 10mM KA. The recordings were obtained at various membrane potentials between -60 and +60mV in 20mV steps in the control solution containing 0.25μM TTX. B: I-V relationship of the KA-response in A. C: effect of spermine on KA-response. control (C1), during bath application of 1mM spermine (C2) and after wash out (C3).

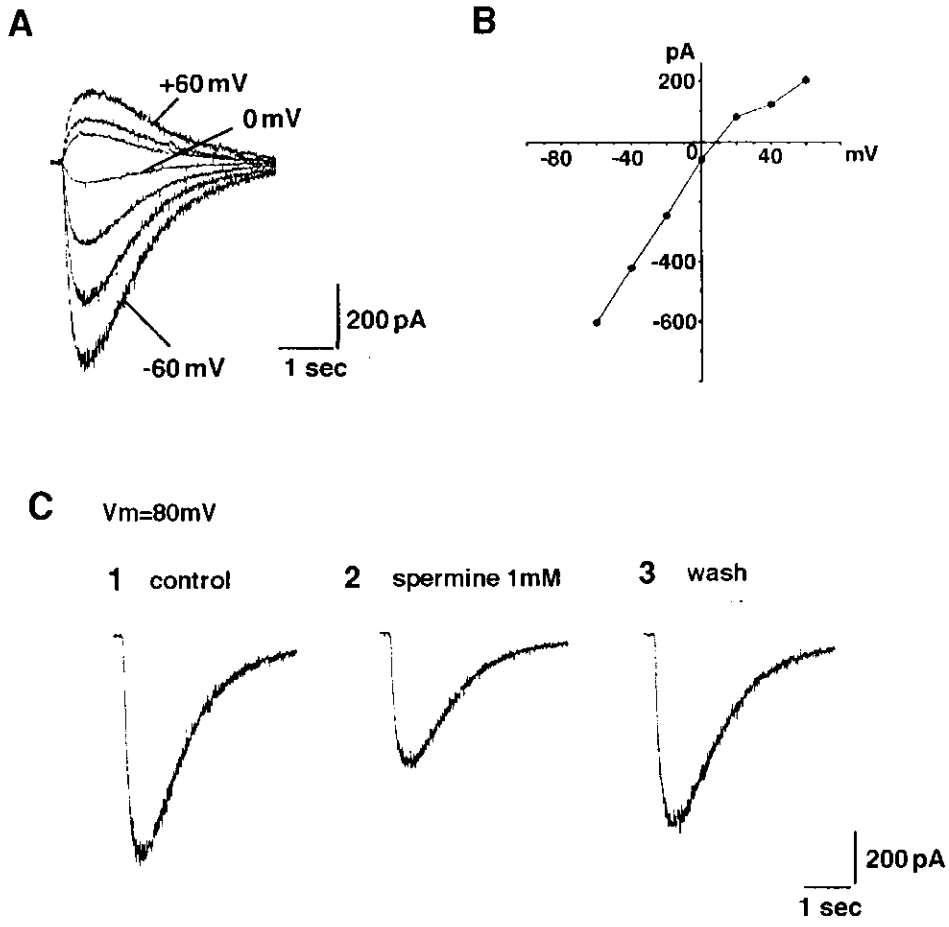

Figure II-2. Inwardly rectifying KA-response.

A: current responses to pressure applied 10mM KA. The recordings were obtained at various membrane potentials between -60 and +60mV in 20mV steps in the control solution containing 0.25μM TTX. B: I-V relationship of the KA-response in A. C: effect of spermine on KA-response. control (C1), during bath application of 1mM spermine (C2) and after wash out (C3).

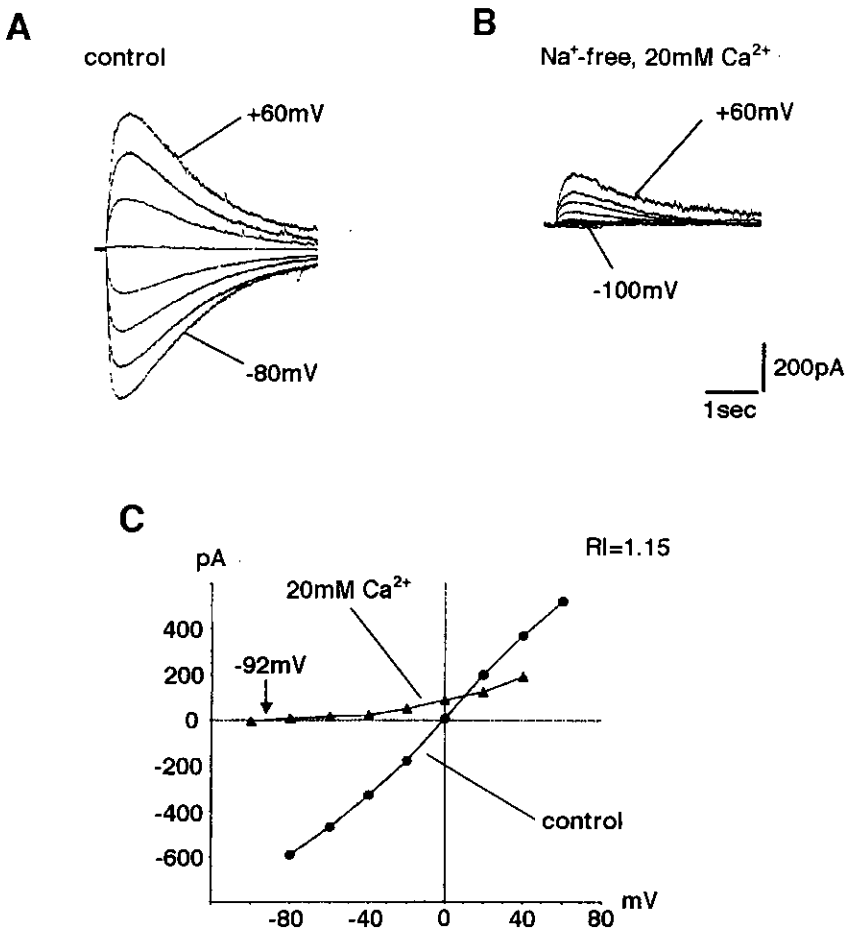

Figure II-3. Ca^{2+} permeability of AMPA receptors in a neuron with outwardly rectifying KA-response.

A and B: current responses to pressure applied 10mM KA. The recordings were obtained at various membrane potentials between -100 and +60mV in 20mV steps under presence of 0.25μM TTX. Recordings in control solution (A) and high Ca^{2+} solution (Na^{+}-free, 20mM Ca^{2+}). C: I-V relationship of the KA-response in A and B. The RI value in the control solution was 1.15.

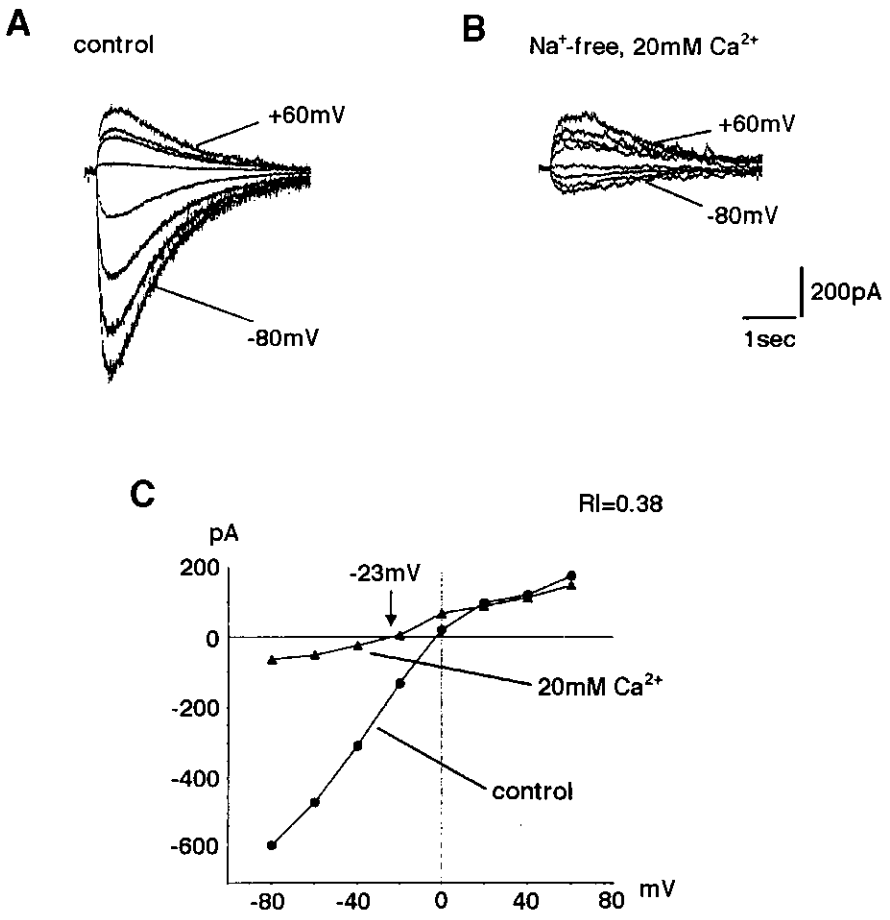

Figure II-4. Ca^{2+} permeability of AMPA receptors in a neuron with inwardly rectifying KA-response.

A and B: current responses to pressure applied 10mM KA. The recordings were obtained at various membrane potentials between -80 and +60mV in 20mV steps under presence of 0.25μM TTX. Recordings in control solution (A) and high Ca^{2+} solution (Na^{+}-free, 20mM Ca^{2+}). C: I-V relationship of the KA-response in A and B. The RI value in the control solution was 0.38.

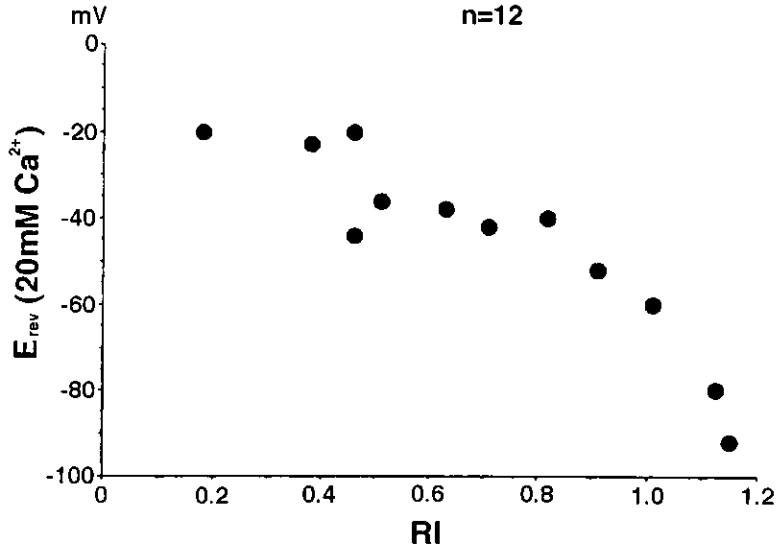

Figure II-5. Scatter plots of reversal potentials of KA-responses in high Ca^{2+} solution against RI values in control solution.

The reversal potentials were obtained from I-V relationships in the solution containing 20mM Ca^{2+} and no Na^{+}. The RI values were obtained from I-V relationships in the control solution. Note that the reversal potential is a indicator of Ca^{2+} permeability and lager value of reversal potential means higher Ca^{2+} permeability.

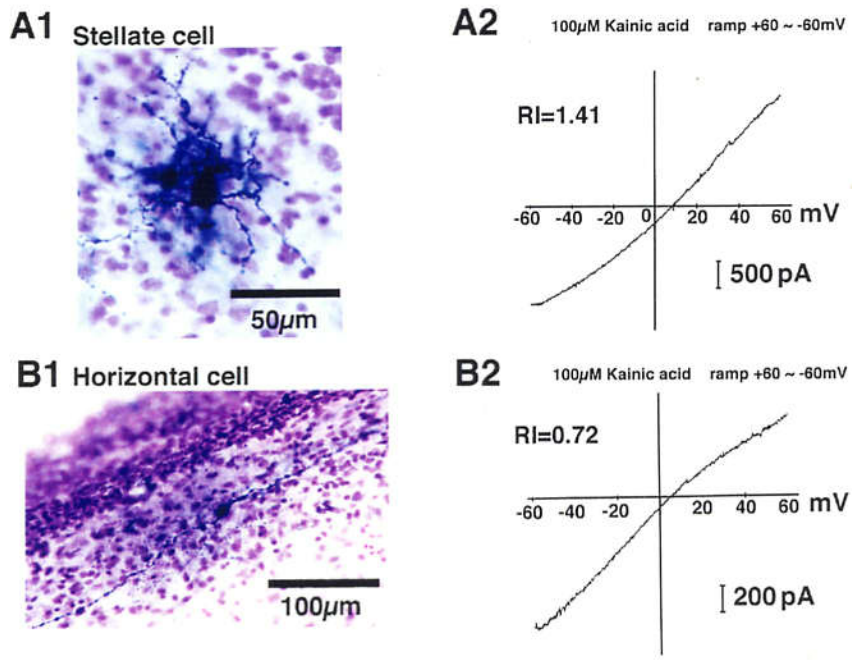

Figure II-6. KA-response of a stellate cell and a horizontal cell

A: photomicrograph of a stellate cell (A1) and I-V relationship of KA-response recorded from the cell (A2). B: photomicrograph of a horizontal cell (B1) and I-V relationship of KA-response recorded from the cell (B2).

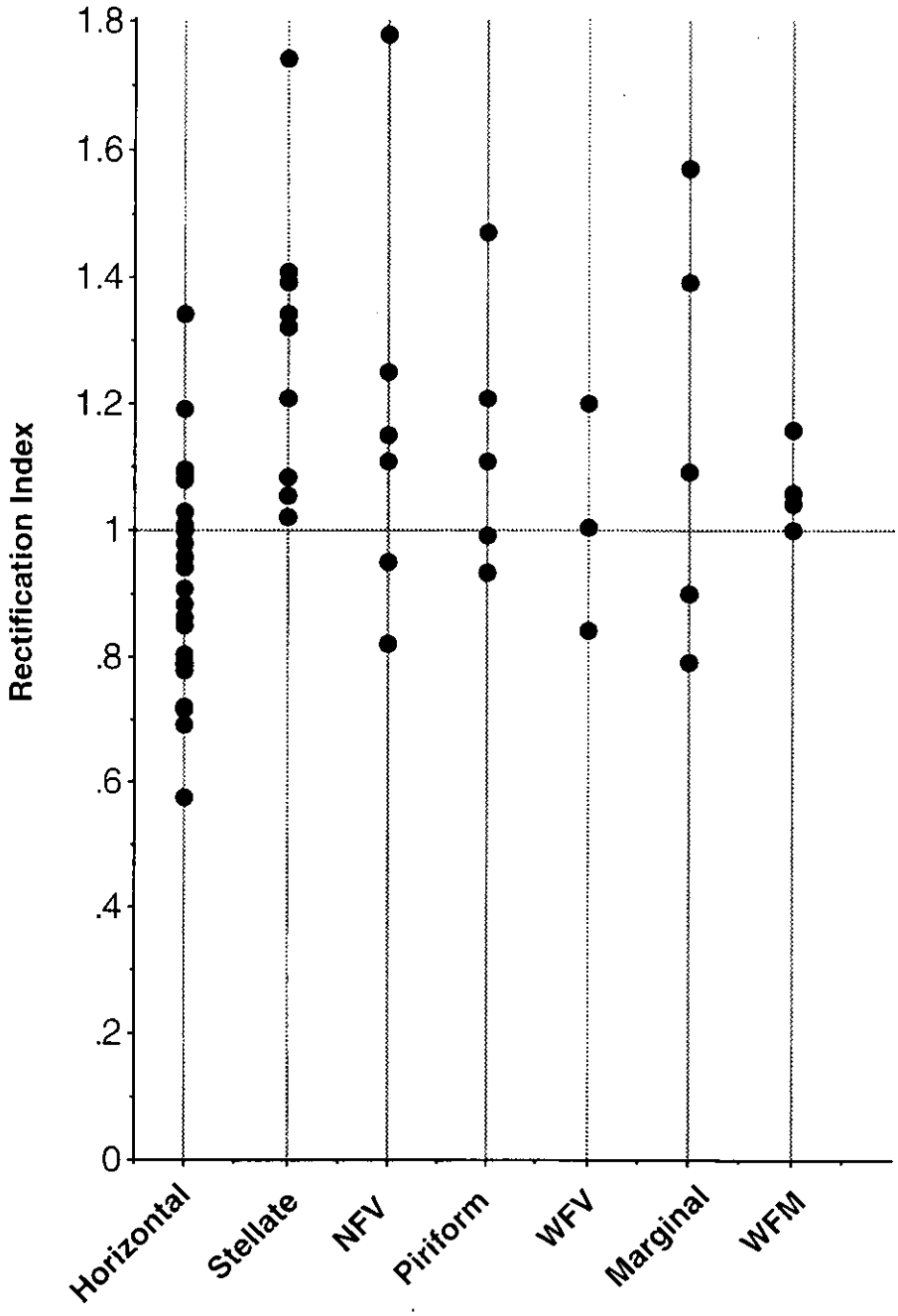

Figure II-7. Correlation between RI value and morphology.

Plots of RI values against morphology. I-V relationships were obtained from current responses to voltage ramps (+60~-60 or -70mV) in solution containing 10-100μM KA, or current responses to pressure applied 10mM KA at various membrane potentials. All recordings were obtained under presence of 0.25–0.5μM TTX. NFV: naroow field vertical cells. WFV: wide field vertical cells. WFM: wide field multipolar cell.

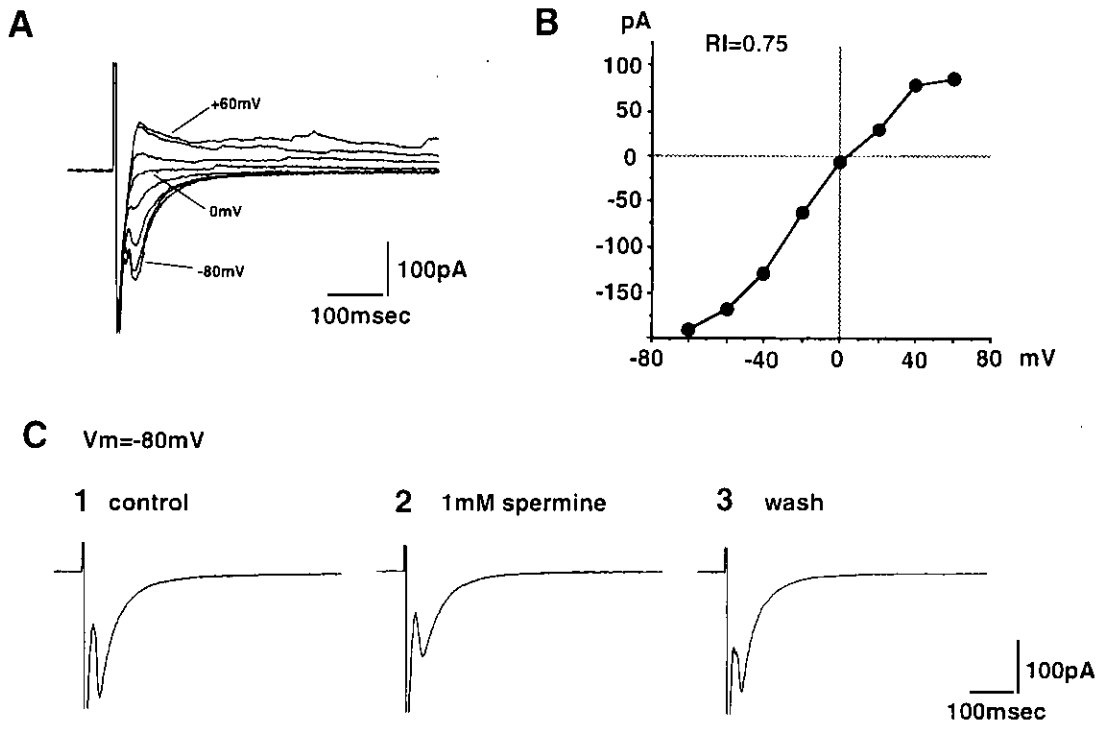

Figure II-8. Inwardly rectifying, spermine-sensitive EPSCs.

A: EPSCs recorded from a SC superficial layer neuron at various membrane potentials between +60 and -80mV in 20mV steps in solution containing 10μM bicuculline and 50μM APV. B: I-V relationship of the EPSCs in A. C: effect of spermine on the EPSCs. Control (C1), during bath application of 1mM spermine (C2) and after wash out (C3).

Chapter III

Organization of inhibitory synapses; Pre- and post-synaptic roles of $GABA_B$ Receptors

Summary

To elucidate the action of $GABA_B$ receptors in the superficial layer of the rat superior colliculus (SC), we tested the effect of specific $GABA_B$ receptor agonist, baclofen, on neurons in slices of rat (PND 16-22) superior colliculus using whole-cell patch clamp technique. Bath application of baclofen (10–30μM) elicited hyperpolarization due to an outward current in neurons including narrow field vertical cells, stellate cells, and wide field vertical cells. The reversal potential of the baclofen-induced current was nearly equal to the equilibrium potential of potassium calculated from Nernst equation, suggesting that $GABA_B$ receptors activated the potassium conductance. Application of baclofen also suppressed both EPSCs and IPSCs evoked by electrical stimulation of adjacent region of recorded cells. Furthermore, all these effect of baclofen was antagonized by application of specific $GABA_B$ receptor antagonist, CGP55845A (0.1–1 μM). Baclofen had no effect on current responses elicited by bath application of 10μM kainic acid or 5μM muscimol under the presence of 0.5 μM tetrodotoxin, suggesting that suppression of synaptic currents occurred at the presynaptic terminal. All the above results have clarified the presynaptic and postsynaptic function of $GABA_B$ receptors: activation of $GABA_B$ receptors at the postsynaptic membrane cause hyperpolarization and activation of those at presynaptic terminal suppresses the synaptic transmission at both glutamatergic and GABAergic synapses. These effects could be observed in a wide variety of cell types in the superficial layer of the SC.

Introduction

In the superficial layer of the SC, particularly in the SGS, there are high density of GABAergic inhibitory neurons. Mize (1992) described that three types of neurons in the SGS (horizontal, piriform and stellate cells) are GABAergic based on his observation of morphology of soma and proximal dendrites of cells stained with antibody to GABA. GABA concentration in the SGS is amongst the highest found in the central nervous system, and the GABA level in the SO was only half that of the concentration in the SGS, however, still higher than that in lower SC layers (Okada, 1993). The activity of GAD, a GABA synthesizing enzyme, also parallels the GABA levels in each layer (Okada, 1993). In addition to the high amount of GABA and GABAergic neurons in the SC superficial layer, functional significance of GABAergic inhibition in the SGS have been reported in a study by Binns and Salt (1997). In their study, they reported that iontophoretic injection of bicuculline, a $GABA_A$ receptor antagonist, into rat SC reduced surround inhibition of visual responses, while injection of CGP35348, a $GABA_B$ receptor antagonist, reduced response habituation.

Thus, the GABAergic inhibition is likely to play an important role on modulation of visual responses of neurons in the SC superficial layer. However, its action at the cellular level is largely unknown, especially with regard to $GABA_B$ receptor-mediated inhibition. In the superficial layer of the SC, there are a large amount of $GABA_B$ receptors as have been indicated by autoradiographic studies (Chu et al., 1990; Bowery et al., 1987). Previous studied have investigated the effects of baclofen on the field potentials elicited by electrical stimulation of optic fibers in the guinea pig SC (Arakawa and Okada, 1988) and the frog optic tectum (Sivilotti and Niatri, 1988) slices. Although they found baclofen-induced inhibition of the field potential, the

detailed mechanisms and the functions of the $GABA_B$ receptor-mediated inhibition have not been known. The functional significance of $GABA_B$ receptors in the nervous system have created considerable interest in recent years. $GABA_B$ receptors differ fundamentally from $GABA_A$ receptor channels. In contrast to $GABA_A$ receptors, $GABA_B$ receptors require a G-protein, are located at pre- and/or post-synaptic membrane, and are coupled to various K^+ and Ca^{2+} channels presumably through both a membrane delimited pathway and a pathway involving second messengers (for review see Kuriyama et al., 1993; Misgeld et al., 1995; Nicoll et al., 1990).

In the present study, we investigated the effect of baclofen to individual neurons in slices of rat SC using whole-cell patch clamp technique. As the first step to understand the mechanisms and the functions of $GABA_B$ receptor-mediated inhibition in the SC superficial layer, we focused on the location of the $GABA_B$ receptors. The present results suggest that the action of $GABA_B$ receptors at both post- and pre-synaptic site in the superficial layer of the rat SC.

Methods

The methods employed in this study were in general similar to those described in chapter I and II of this thesis, except for several points. Frontal slices (300μm thick) of the SC were prepared from 16- to 22-day-old Wistar rats following ether anesthesia. The slices were incubated at room temperature for > 1 hour in control Ringer's solution before recording. Whole-cell patch clamp recordings (Edwards et al., 1989; Hamill et al., 1981) were obtained from neurons using visual control of the patch pipettes. The control Ringer's solution contained (mM) : 125 NaCl, 2.5 KCl, 2 $CaCl_2$, 1 $MgCl_2$, 26 $NaHCO_3$, 1.25 NaH_2PO_4, 25 glucose, and continuously bubbled with 95% O_2 and 5% CO_2 (pH 7.4). Two types of intracellular solutions with different composition were used. The one contained (mM) : 140 K-gluconate, 20 KCl, 0.2 EGTA, 2 $MgCl_2$, 2 Na_2ATP, 0.5 NaGTP, 10 HEPES, 0.1 spermine, pH 7.3. In some cases, K-gluconate was substituted for KCl. The other contained (mM) : 120 Cs-gluconate, 20 CsCl, 10 EGTA, 2 $MgCl_2$, 2 Na_2ATP, 10 HEPES, 0.1 spermine, 5 Qx-314, pH 7.3. To stain the recorded neurons, biocytin (5mg/ml, Sigma, St. Louis, MO) and lucifer yellow (1mg/ml, Sigma) were dissolved in each solution. To obtain the current-voltage (I-V) relationship of the baclofen responses, the membrane potential was ramped from -50 to -120 mV and then shifted from -120 to –50 mV again at a rate of 140 mV/s. The current records in the former phase were used. The I-V curve was obtained by subtracting the current recorded in the standard Ringer's solution from that obtained during bath application of baclofen. Excitatory postsynaptic currents (EPSCs) and inhibitory postsynaptic currents (IPSCs) were evoked by electrical stimulation (cathodal square wave current pulses, 2.7–11.2 μA, 0.2 ms duration) with a glass pipette containing 2M NaCl solution placed about 100μm away from the recorded neuron.

After recording, slices were fixed with 4% paraformaldehyde and recorded neurons were visualized by staining with biocytin (Horikawa and Armstrong, 1988), using ABC method. Baclofen, kainic acid and muscimol were obtained from Sigma. 6-Cyano-7-nitroquinoxaline-2,3-dione (CNQX), 2-amino-5-phosphonovaleric acid (APV) and bicuculline were from RBI (Natick, MA). Tetrodotoxin (TTX) was from Sankyo (Tokyo, Japan). CGP55845A was a gift from Novartis (Basel, Switzerland). All drugs were bath applied.

Results

Postsynaptic effect of baclofen

Action of $GABA_B$ receptors on the postsynaptic membrane was tested by bath application of baclofen (10–30 μM) under the presence of 0.25–0.5 μM TTX in neurons in the superficial layer of the SC.

Figure. III-1A shows an example of the effect of bath application of baclofen (10μM, 120sec) elicited marked hyperpolarization (Fig. III-1Aa). The baclofen-induced hyperpolarization was completely suppressed when CGP55845A (1μM), an antagonist of $GABA_B$ receptors, was added into the bath during the application of baclofen (Fig. III-1Ab). Baclofen-induced hyperpolarization was observed in 22 of 25 cells tested, and the effect was antagonized by CGP55845A (0.1–1μM) in 11 of 11 cells tested.

Figure III-1B shows the outward current response induced by application of baclofen (30μM) recorded in another neuron at the holding potential of –50 mV. The rapid downward deflections are current responses to voltage ramps from –50 to –120mV. Bath application of baclofen elicited an outward current which was associated with an increase in membrane conductance as indicated by increases in the current response to the voltage ramp (Fig. III-1B). Bath application of baclofen thus elicited an outward current in 9 of 13 cells tested.

To know the substrate of the membrane conductance changed by baclofen, we investigated the reversal potential (E_{rev}) of the baclofen-induced current by ramping holding potential from –50 mV to –120 mV. Figure III-2A shows an example of recordings from the neuron in Fig. III-1B, where the E_{rev} for baclofen-induced current was –102.5mV. The average value was –105.5 ± 6.6 mV (mean ± S.D., n=4), which was close to equilibrium potential for potassium calculated from Nernst equation (–106.8mV, in 2.5 mM

potassium at 25℃). Then we measured the E_{rev} for baclofen-induced current in high potassium extracellular solution (12.5 mM). Figure III-2B shows an example of recordings in this conditions, and the E_{rev} for baclofen-induced current was –61.6 mV. In this conditions the average value of E_{rev} was –65.0 ± 7.6 mV (mean ± S.D., n=4), which was also close to the equilibrium potential for potassium calculated from Nernst equation (–65.5mV). Figure III-2C shows plots of E_{rev} for baclofen-induced current against the extracellular potassium concentration. The E_{rev} values are distributed near the line which indicates potassium equilibrium potential expected from Nernst equation. These results have shown that baclofen elicited an increase in potassium conductance in SC superficial layer neurons.

Figure III-3 shows examples of lucifer yellow-filled neurons which exhibited hyperpolarization caused by baclofen. Baclofen elicited hyperpolarization in narrow field vertical cells (n = 8/9), stellate cells (n = 2/2) and wide field vertical cells (n = 3/3).

Presynaptic effect of baclofen

We next investigated whether $GABA_B$ receptors had any actions at the presynaptic terminals of either excitatory and inhibitory synapses in the superficial layer of rat SC. We tested the effect of bath application of baclofen (10–20μM) on electrically evoked excitatory synaptic currents (EPSCs) and inhibitory synaptic currents (IPSCs). To eliminate baclofen-induced potassium current in the post-synaptic membrane, potassium-free intracellular solution (Cs-gluconate) was used.

Action at the glutamatergic excitatory synapse

As exemplified in figure III-4A and B, postsynaptic currents evoked by electrical stimulation under the presence of 10 μM bicuculline were

suppressed by baclofen added into the bath. This effect of baclofen (10μM) was antagonized by CGP55845A (0.1μM). The postsynaptic currents were almost completely suppressed by CNQX (10μM) and APV (50–100μM), indicating that the postsynaptic currents were glutamatergic excitatory postsynaptic currents (EPSCs) and mediated by AMPA and NMDA-type glutamate receptors. Similar effects of baclofen (10–20μM) and CGP55845A (0.1μM) were observed in all cells tested (n=4 and 4, respectively).

These results suggest that $GABA_B$ receptors exist at the excitatory presynaptic terminals of the neurons in the superficial layer of the rat SC, and activation of these receptors resulted in suppression of excitatory synaptic transmission. However, an alternative mechanism could mediate the suppression. It was possible that baclofen activated postsynaptic $GABA_B$ receptors and then directly inhibited glutamate receptors on the postsynaptic membrane through some intracellular mechanisms. To exclude this possibility, we directly activated postsynaptic AMPA-type glutamate receptors by bath application of 10μM kainic acid and examined the effect of baclofen on kainic acid-induced current. As shown in figure III-4C, amplitude of inward current induced by bath application of kainic acid in the control solution in the presence of 0.5 μM TTX was not altered by additional application of baclofen (n=5). These results strongly suggested that $GABA_B$ receptors presumably located at the presynaptic terminals suppressed the excitatory synaptic transmission at the glutamatergic synapses in the superficial layer of the SC.

Action at the GABAergic inhibitory synapse

As shown in figure III-5A and B, postsynaptic currents evoked by electrical stimulation under the presence of 10μM CNQX and 50 – 100μM

APV were suppressed by application of 20 μM baclofen in the extracellular solution, and application of 0.1 μM CGP55845A released the synaptic currents from suppression by baclofen. The synaptic currents were almost completely suppressed by bicuculline (10μM, Fig. III-5B). Thus, the postsynaptic currents were inhibitory postsynaptic currents (IPSCs) mediated by $GABA_A$ receptors and $GABA_B$ receptors suppressed the synaptic transmission at the GABAergic inhibitory synapses. In the present study, the IPSCs by activation of $GABA_A$ receptors were recorded as inward currents at the holding potential of –80mV, since the reversal potential of the Cl^- conductance was –43 mV in the present experimental arrangement ($[Cl^-]_i$ =24 mM and $[Cl^-]_o$ = 133.5mM). Similar effect of baclofen and CGP55845A were observed in all cells tested (n=13 and 3, respectively). These results suggest that $GABA_B$ receptors exist at the inhibitory presynaptic terminals of the neurons in the superficial layer of the SC, activation of these receptors resulted in suppression of inhibitory synaptic transmission.

To exclude the possible involvement of the postsynaptic effect, we directly activated postsynaptic $GABA_A$ receptors by bath application of 5–10μM muscimol and examined the effect of baclofen on muscimol-induced current. As shown in figure III-5C, baclofen (10μM) had no effect on currents elicited by muscimol (n=5). These results strongly suggested that $GABA_B$ receptors at the presynaptic terminals suppressed the inhibitory synaptic transmission at the GABAergic synapses in the superficial layer of the SC.

Discussion

The present study has shown that $GABA_B$ receptor agonist, baclofen elicits hyperpolarization in post-synaptic neurons by an increase in potassium conductance. Furthermore, the present study demonstrate d that both glutamatergic EPSCs and GABAergic IPSCs were suppressed by baclofen in various types of neurons in the superficial layer. Since baclofen had no effect on post-synaptic currents induced by kainic acid or muscimol, suppression of EPSCs and IPSCs may be caused by pre-synaptic effects of baclofen..

$GABA_B$ receptors are known to be located at pre-synaptic terminals and/or post-synaptic membrane (for review see Kuriyama et al., 1993; Misgeld et al., 1995; Nicoll et al., 1990). In the superficial layer of the SC, previous studied have reported that baclofen suppresses the field potentials elicited by electrical stimulation of optic fibers in the guinea pig SC (Arakawa and Okada, 1988) and the frog optic tectum (Sivilotti and Niatri, 1988) slices, although these studies have not investigated the site of action of baclofen. Autoradiographic studies have indicated that the $GABA_B$ receptors are abundant in the superficial layer of the SC (Chu et al., 1990; Bowery et al., 1987). The $GABA_{B1}$ receptor mRNA is also present in the superficial layer of the SC as indicated in an in situ hybridization study (Lu et al., 1999). However, all these previous studies have not demonstrated the subcellular distribution of $GABA_B$ receptors in a neuronal membrane. The present results suggest that $GABA_B$ receptors exist at both postsynatic membrane and presynaptic terminals and mediate both postsynaptic and presynaptic inhibition in the superficial layer of the rat SC.

The results of the present study also indicated that baclofen elicits hyperpolarization in at least three morphologically different types of cells,

narrow field vertical cells, stellate cells and wide field vertical cells.. Although morphological classification of the neurons in which evoked EPSCs and IPSCs were recorded was not identified in the present study, suppression of the EPSCs and the IPSCs by baclofen were observed in all the cases tested. Thus, we could not demonstrate any specificity for post-synaptic cell type in the present study, suggesting that $GABA_B$ receptor-mediated inhibition is involved in synaptic transmission onto wide range of morphologically different neurons and may affects various aspects of information processing in the superficial layer of the SC.

In the neocortex and the hippocampus, various studies have suggested that $GABA_B$ autoreceptors on the pre-synaptic terminals are involved in regulation of long-term and short-term synaptic plasticity, such as long-term potentiation (LTP; Davies et al., 1991), paired-pulse facilitation of EPSPs which is associated with depression of superimposed IPSPs (Nathan and Lambert, 1991) and paired-pulse depression of IPSPs (Deisz and Prince, 1989; Davies et al., 1991; Fukuda et al., 1993; Lambert and Wilson, 1993; Nathan and Lambert, 1991). Short-lasting heterosynaptic depression of excitatory synaptic transmission mediated by $GABA_B$ receptors located on pre-synaptic terminals was also reported (Isaacson et al., 1993). Furthermore, interactions between the short-term synaptic plasticity and slow IPSPs mediated by post-synaptic $GABA_B$ receptors give rise to complex net effect (Buonomano et al., 1998). In the superficial layer of the SC, the involvement of $GABA_B$ receptors in plastic events are largely unknown. Okada and his colleagues have reported that induction of LTP of field EPSPs is regulated through GABAergic mechanism, and they suggested the involvement of $GABA_A$ receptors (Hirai et al., 1993; Hirai and Okada, 1993; Okada, 1993). Although they did not examine the involvement of $GABA_B$ receptors, involvement of $GABA_B$ receptors cannot be excluded. More

recently, it has been suggested that $GABA_B$ receptors at least partly contribute to paired-pulse depression (Platt and Withington, 1997a) and response habituation (Platt and Withington, 1997b) of field EPSPs in guinea pig slice preparations of the SC. Contribution of $GABA_B$ receptors in habituation of response to repetitive visual stimuli is also reported in intact animals (Binns and Salt, 1997). However, understanding of synaptic mechanisms by which $GABA_B$ receptors mediate these plastic events are still lacking. Because the present study suggests that $GABA_B$ receptors are involved in synaptic transmission onto various types of neurons through both post- and pre-synaptic mechanisms, it is highly likely that several mechanisms contribute to the plastic events in parallel and/or via mutual interactions. More detailed analysis about action of $GABA_B$ receptors is needed, and our approach, i.e. recordings in morphologically identified individual neurons, will provide essential information to understand the action of $GABA_B$ receptors in the information processing in the local circuits of the superficial layer in the SC.

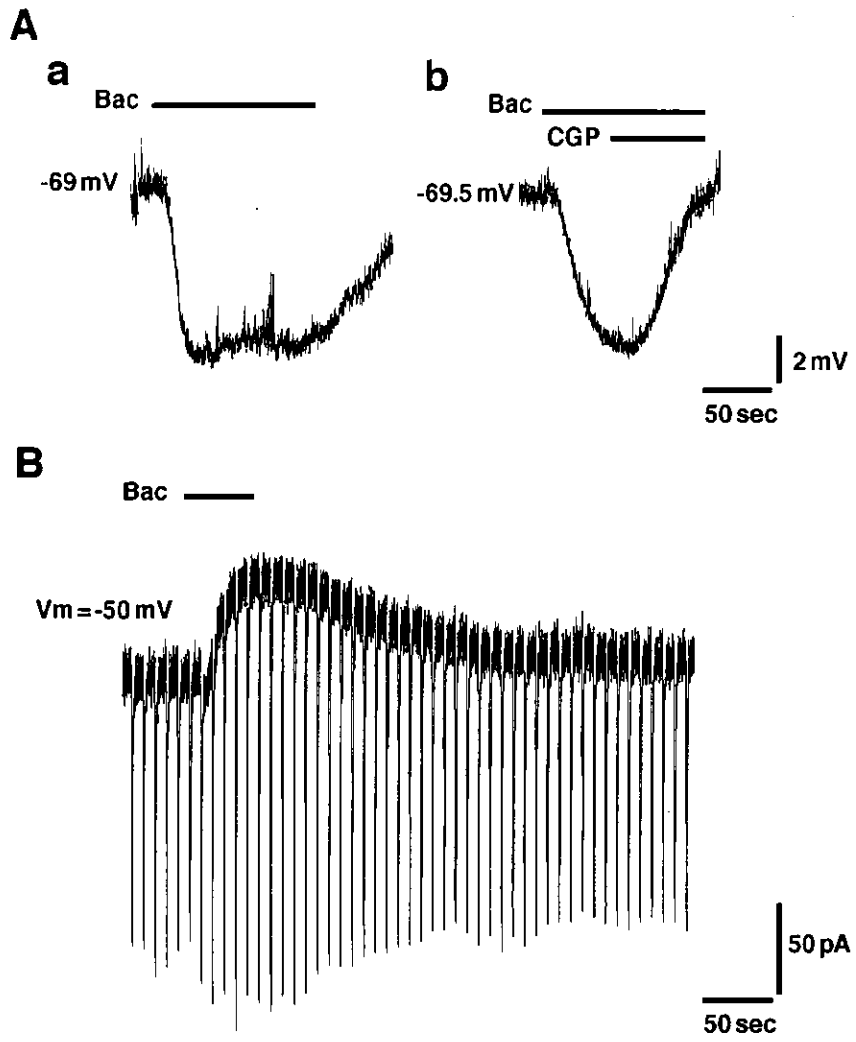

Figure III-1. Post-synaptic effect of baclofen.

A: current clamp recordings from a neuron in the superficial layer of the SC. Aa: bath application of 10μM baclofen (Bac) elicited hyperpolarization. Ab: baclofen-induced hyperpolarization was suppressed by application of 1μM CGP55845A (CGP). B: current response to application of 30μM baclofen obtained from another neuron. The rapid downward deflections are current responses to voltage ramps from -50mV to -120mV.

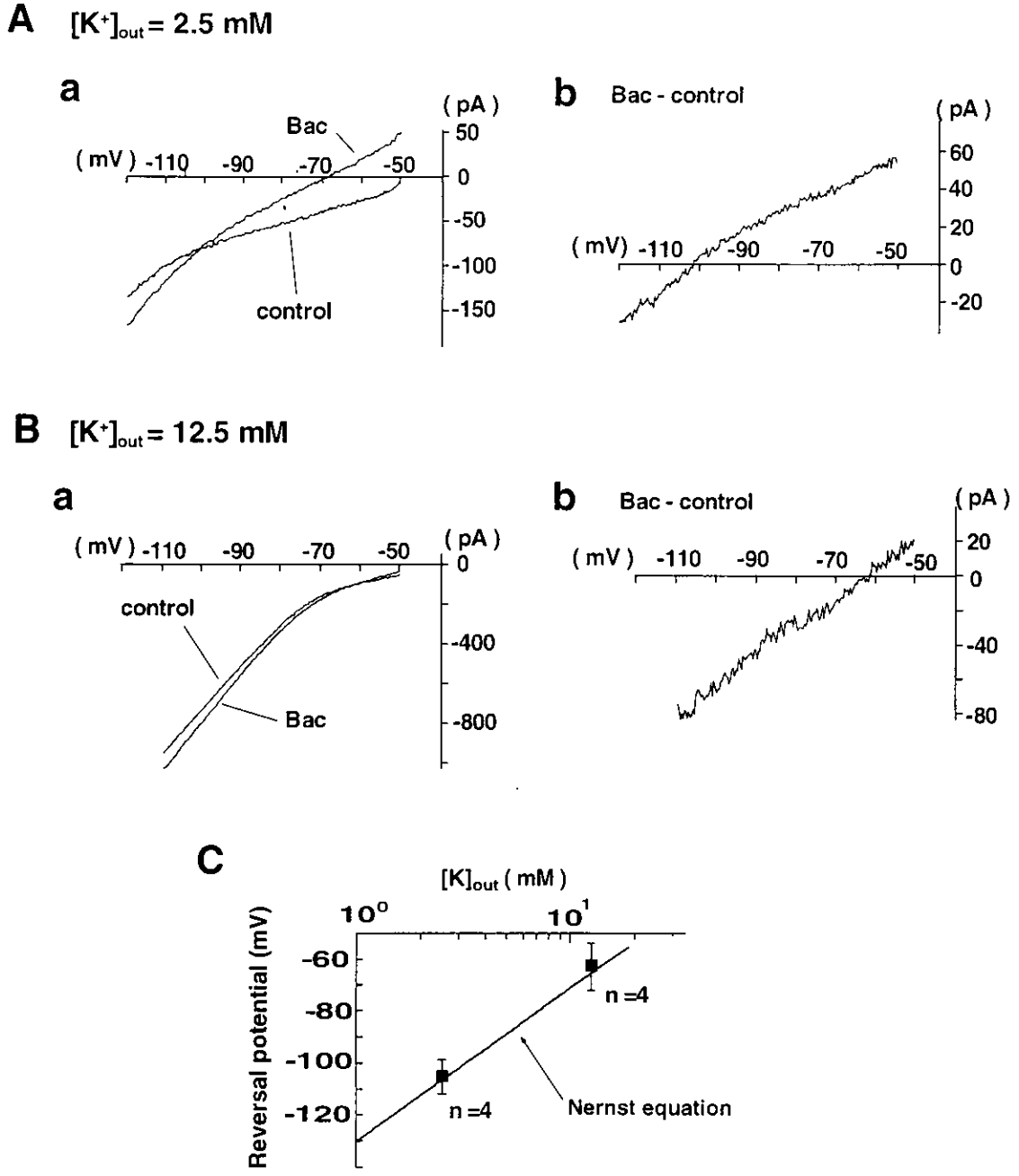

Figure III-2. Reversal potentials of baclofen-induced current in the extracellular solutions containing 2.5 and 12.5mM K^+.

A: recordings from a SC superficial layer neuron in the solution containing 2.5mM K^+. Aa: current-voltage relationships during hyperpolarizing voltage ramps from -50 to -120mV in the control and during bath application of 30μM baclofen (bac). Ab: subtraction of the two current responses, control and bac, in Aa. The reversal potential was -102.5mV. B: recordings from a SC superficial layer neuron in the solution containing 12.5mM K^+. The reversal potential of baclofen-induced current was -61.6mV. Details as in A. C: plots of mean values of the reversal potential in the two condition against the concentration of K^+ in the extracellular solution. The solid line indicates the K^+ equilibrium potential calculated from Nernst equation. The horizontal axis is indicated as logarithmic scale.

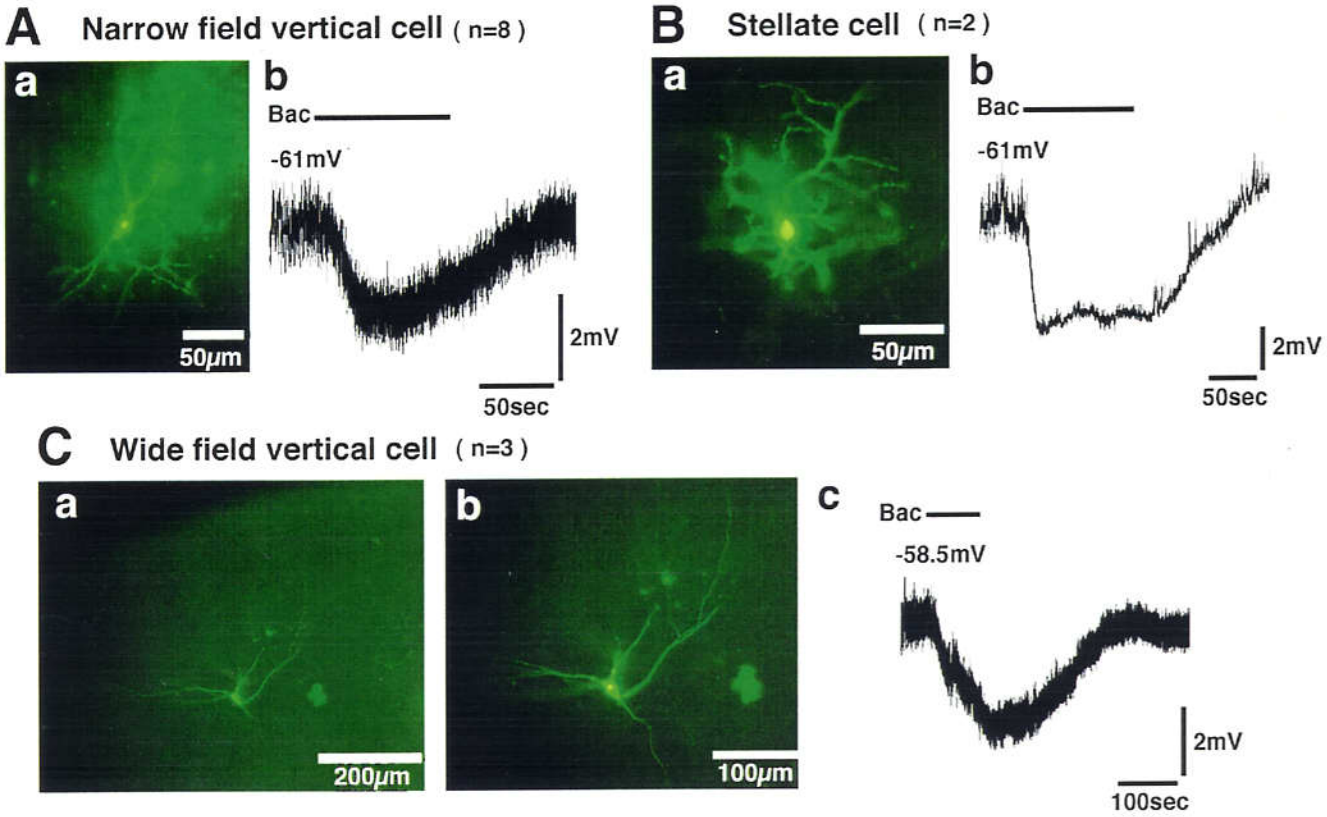

Figure III-3. Neurons which showed baclofen-induced hyperpolarization.

A: photomicrograph of a lucifer yellow-filled narrow field vertical cell (Aa) and the voltage response to bath applied baclofen (Ab). B: photomicrograph of a lucifer yellow-filled stellate cell (Ba) and the voltage response to bath applied baclofen (Bb). C: photomicrograph of a lucifer yellow-filled wide field vertical cell (Ca and b) and the voltage response to bath applied baclofen (Cc).

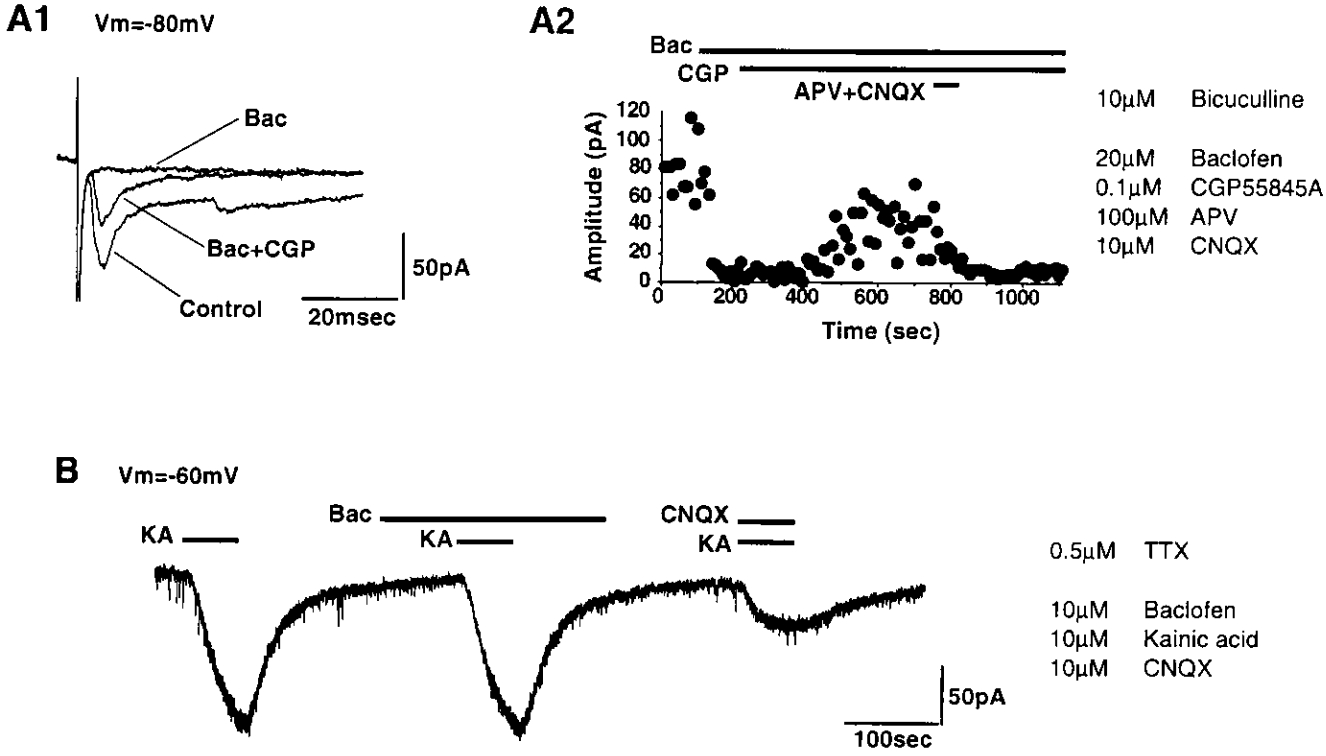

Figure III-4. Effect of baclofen on evoked EPSCs.

A: electrically evoked EPSCs under presence of 10μM bicuculline. A1: effect of baclofen (bac) and CGP55845A (CGP) on the EPSCs. Each trace is average of five recordings. A2: time course of the effect of drugs (indicated at right) on the EPSCs. B: effect of baclofen and CNQX on currents elicited by bath application of 10μM kainic acid. TTX (0.5μM) was bath applied throughout the recording.

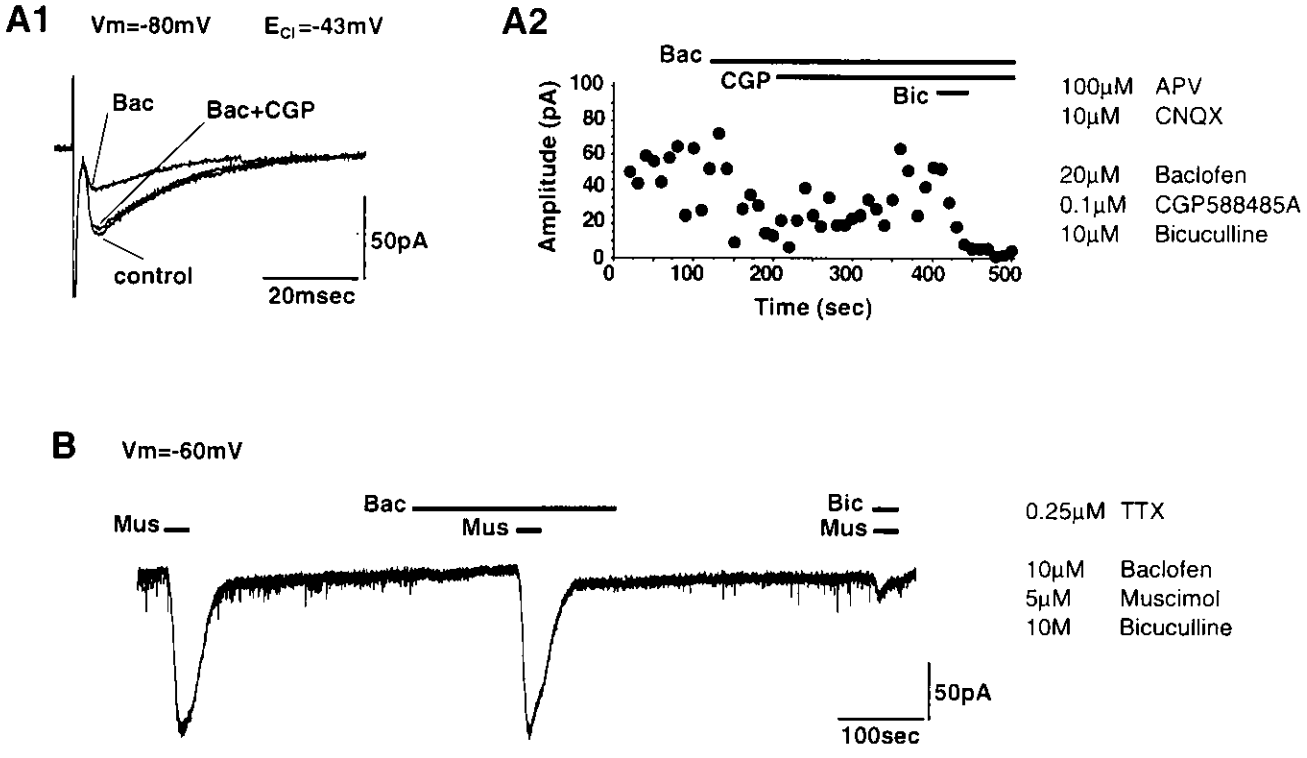

Figure III-5. Effect of baclofen on evoked IPSCs.

A: electrically evoked IPSCs under presence of 100μM APVand 10μM CNQX. A1: effect of baclofen (bac) and CGP55845A (CGP) on the IPSCs. Each trace is average of five recordings. A2: time course of the effect of drugs (indicated at right) on the IPSCs. B: effect of baclofen and bicuculline on currents elicited by bath application of 10μM kainic acid. TTX (0.25μM) was bath applied throughout the recording.

General Discussion

In this study, we investigated the electrophysiological and morphological properties of neurons in the superficial layer of rat SC, using whole-cell patch clamp recording technique. The results of the present study indicate that there are wide variety of neurons with respect to the membrane properties, expression of AMPA receptor subtype and morphology. In contrast to these properties, we could not demonstrate any specificity for post-synaptic cell type in the present study, although we did not identify the presynaptic neurons.

In the neocortex and the hippocampus, previous studies have reported that firing properties are well correlated with specific morphological characteristics and function (excitatory or inhibitory, interneuron or projection neuron) of the cells (Connors and Guttnick, 1990; Kawaguchi et al., 1987; Kawaguchi and Kubota, 1997). In contrast, in the superficial layer of the SC, results of the present study suggest that firing properties and morphological characteristics are not correlated. All morphologically classified neuronal subclasses were heterogeneous with respect to firing properties, and except for marginal cells, all groups included both regular spiking neurons and burst spiking neurons. Such difference also seems to be true of expression pattern of subtype of AMPA receptors and specific cell marker protein such as parvalbumin. Most neurons which express the Ca^{2+}-permeable AMPA receptors are GABAergic and express parvalbumin in the neocortex and the hippocampus (Bochet et al., 1994; Jonas et al., 1994; Kondo et al., 1997; Leranth et al., 1996). In the superficial layer of the SC, horizontal cells, which contain substantial population of neurons expressing Ca^{2+}-permeable AMPA receptors, are supposed to be GABAergic (Mize, 1992). Although parvalbumin immunoreactive horizontal cells were observed (Cork

et al., 1998), these cells are not the major population among parvalbumin immunoreactive cells in the superficial layer of the rat SC (e.g., Cork et al., 1998; Illing et al., 1990). Thus, it may be necessary to consider another rule about the correlation between the electrophysiological and morphological properties in the superficial layer of the rat SC from that established in the neocortex and hippocampus. At this moment, the situation in the SC superficial layer are still confusing. For example, although horizontal cells, piriform cells and stellate cells are supposed to be GABAergic (Mize, 1992), we do not know whether all these cells are GABAergic because the identification have been done only based on morphology of soma and proximal dendrites of GABA immunopositive cells. In addition, Mooney et al (1988b) demonstrated that the major population of neurons projecting to the LP and dLGN are wide field vertical cells and narrow field vertical cells (including piriform cells according to our criteria), and stellate cells and horizontal cell are also contained both populations in the superficial layer of the hamster SC. Thus, we can not safely identify neurons as projection neuron and/or interneuron simply based on the morphology at this moment.

GABAergic systems in the superficial layer of the SC bear fundamental and complex functions. GABAergic inhibition play a siginificant role in surround inhibition and response habituation (Binns and Salt, 1997), that is the most characteristic properties of SC superficial layer neruons. Several in vitro studies have demonstrated that GABAergic action regulate long-term and short-term plasticity (Hirai et al., 1993; Hirai and Okada, 1993; Okada, 1993; Platt and Withington, 1997a, 1997b). Excitatory action of low concentration of GABA have been also reported, and this action is likely to be mediated by $GABA_C$ receptors (Arakawa and Okada, 1988; Pasternack et al., 1999). However, detailed mechanisms of these functions are mostly unknown, at least partly because of the limitation of the

recording technique. All these in vitro studies employed extracellular recording technique, and observed the summation of processes which occur in parallel and may interact each.

Thus, most fundamental information essential to understand the mechanisms of information processing in the superficial layer of the SC is still lacking. Nevertheless, the superficial layer of the SC is an attractive and suitable system to investigate the mechanisms of information processing in the nervous system. There is an exact map of contralateral visual field in the superficial layer of the SC, and direct coupling to motor system through connection to the deeper SC layers will enable us to verify the knowledge obtained in vitro experiments in behavioral context in future work. To elucidate the mechanisms of information processing in the local circuits of the SC superficial layer, we have to know the properties of individual neurons and the mechanisms of their mutual interaction, and more detailed analysis is needed. Our approach, i.e. recordings in morphologically identified individual neurons, together with combination with other technique, will provide essential information about this issue.

References

Arakawa, T., and Okada, Y. (1988). Excitatory and inhibitory action of GABA on synaptic transmission in slices of guinea pig superior colliculus. Eur J Pharmacol 158, 217-24.

Binns, K. E., and Salt, T. E. (1997). Different roles for $GABA_A$ and $GABA_B$ receptors in visual processing in the rat superior colliculus. J Physiol (Lond) 504, 629-39.

Bochet, P., Audinat, E., Lambolez, B., Crepel, F., Rossier, J., Iino, M., Tsuzuki, K., and Ozawa, S. (1994). Subunit composition at the single-cell level explains functional properties of a glutamate-gated channel. Neuron 12, 383-8.

BoSmith, R. E., Briggs, I., and Sturgess, N. C. (1993). Inhibitory actions of ZENECA ZD7288 on whole-cell hyperpolarization activated inward current (If) in guinea-pig dissociated sinoatrial node cells. Br J Pharmacol 110, 343-9.

Bowery, N. G., Hudson, A. L., and Price, G. W. (1987). GABAA and GABAB receptor site distribution in the rat central nervous system. Neuroscience 20, 365-83.

Buonomano, D. V., and Merzenich, M. M. (1998). Net interaction between different forms of short-term synaptic plasticity and slow-IPSPs in the hippocampus and auditory cortex. J Neurophysiol 80, 1765-74.

Chu, D. C., Albin, R. L., Young, A. B., and Penney, J. B. (1990). Distribution and kinetics of $GABA_B$ binding sites in rat central nervous system: a quantitative autoradiographic study. Neuroscience 34, 341-57.

Connors, B. W., and Gutnick, M. J. (1990). Intrinsic firing patterns of diverse neocortical neurons. Trends Neurosci 13, 99-104.

Cork, R. J., Baber, S. Z., and Mize, R. R. (1998). CalbindinD28k- and parvalbumin-immunoreactive neurons form complementary sublaminae in the rat superior colliculus. J Comp Neurol 394, 205-17.

Cynader, M., and Berman, N. (1972). Receptive-field organization of monkey superior colliculus. J Neurophysiol 35, 187-201.

Davies, C. H., Starkey, S. J., Pozza, M. F., and Collingridge, G. L. (1991).

GABA autoreceptors regulate the induction of LTP. Nature 349, 609-11.

Dean, P., Redgrave, P., and Westby, G. W. (1989). Event or emergency? Two response systems in the mammalian superior colliculus. Trends Neurosci 12, 137-47.

Deisz, R. A., and Prince, D. A. (1989). Frequency-dependent depression of inhibition in guinea-pig neocortex in vitro by $GABA_B$ receptor feed-back on GABA release. J Physiol (Lond) 412, 513-41.

Donnelly, J. F., Thompson, S. M., and Robertson, R. T. (1983). Organization of projections from the superior colliculus to the thalamic lateral posterior nucleus in the rat. Brain Res 288, 315-9.

Edwards, F. A., Konnerth, A., Sakmann, B., and Takahashi, T. (1989). A thin slice preparation for patch clamp recordings from neurones of the mammalian central nervous system. Pflügers Arch 414, 600-12.

Fukuda, A., Mody, I., and Prince, D. A. (1993). Differential ontogenesis of presynaptic and postsynaptic $GABA_B$ inhibition in rat somatosensory cortex. J Neurophysiol 70, 448-52.

Gauss, R., Seifert, R., and Kaupp, U. B. (1998). Molecular identification of a hyperpolarization-activated channel in sea urchin sperm. Nature 393, 583-7.

Geiger, J. R., Melcher, T., Koh, D. S., Sakmann, B., Seeburg, P. H., Jonas, P., and Monyer, H. (1995). Relative abundance of subunit mRNAs determines gating and Ca^{2+} permeability of AMPA receptors in principal neurons and interneurons in rat CNS. Neuron 15, 193-204.

Goldberg, M. E., and Wurtz, R. H. (1972a). Activity of superior colliculus in behaving monkey. I. Visual receptive fields of single neurons. J Neurophysiol 35, 542-59.

Goldberg, M. E., and Wurtz, R. H. (1972b). Activity of superior colliculus in behaving monkey. II. Effect of attention on neuronal responses. J Neurophysiol 35, 560-74.

Gu, J. G., Albuquerque, C., Lee, C. J., and MacDermott, A. B. (1996). Synaptic strengthening through activation of Ca^{2+}-permeable AMPA receptors. Nature 381, 793-6.

Hagiwara, S., and Takahashi, K. (1974). The anomalous rectification and

cation selectivity of the membrane of a starfish egg cell. J Membr Biol 18, 61-80.

Hamill, O. P., Marty, A., Neher, E., Sakmann, B., and Sigworth, F. J. (1981). Improved patch-clamp techniques for high-resolution current recording from cells and cell-free membrane patches. Pflügers Arch 391, 85-100.

Harris, N. C., and Constanti, A. (1995). Mechanism of block by ZD 7288 of the hyperpolarization-activated inward rectifying current in guinea pig substantia nigra neurons in vitro. J Neurophysiol 74, 2366-78.

Hirai, H., and Okada, Y. (1993). Ipsilateral corticotectal pathway inhibits the formation of long-term potentiation (LTP) in the rat superior colliculus through GABAergic mechanism. Brain Res 629, 23-30.

Hirai, H., Tomita, H., and Okada, Y. (1993). Inhibitory effect of GABA (gamma-aminobutyric acid) on the induction of long-term potentiation in guinea pig superior colliculus slices. Neurosci Lett 149, 198-200.

Hollmann, M., Hartley, M., and Heinemann, S. (1991). Ca^{2+} permeability of KA-AMPA--gated glutamate receptor channels depends on subunit composition. Science 252, 851-3.

Horikawa, K., and Armstrong, W. E. (1988). A versatile means of intracellular labeling: injection of biocytin and its detection with avidin conjugates. J Neurosci Methods 25, 1-11.

Huerta, M. .F. and Harting, J. K. (1984). The mammalian superior colliculus: studies of its morphlogy and connections. In : Comparative Neurology of the Optic Tectum, edited by H. Vanegas. New York: Plenum, 1984, p. 687-773.

Humphrey, K. W. (1968). Induction of deciduomata in normal and histamine-depleted rats. Aust J Biol Sci 21, 331-9.

Iino, M., Mochizuki, S., and Ozawa, S. (1994). Relationship between calcium permeability and rectification properties of AMPA receptors in cultured rat hippocampal neurons. Neurosci Lett 173, 14-6.

Iino, M., Ozawa, S., and Tsuzuki, K. (1990). Permeation of calcium through excitatory amino acid receptor channels in cultured rat hippocampal neurones. J Physiol (Lond) 424, 151-65.

Illing, R. B., Vogt, D. M., and Spatz, W. B. (1990). Parvalbumin in rat superior

colliculus. Neurosci Lett 120, 197-200.

Isa, T., Endo, T., and Saito, Y. (1998). The visuo-motor pathway in the local circuit of the rat superior colliculus. J Neurosci 18, 8496-504.

Isa, T., Iino, M., and Ozawa, S. (1996). Spermine blocks synaptic transmission mediated by Ca^{2+}-permeable AMPA receptors. Neuroreport 7, 689-92.

Isa, T., Itazawa, S., Iino, M., Tsuzuki, K., and Ozawa, S. (1996). Distribution of neurones expressing inwardly rectifying and Ca^{2+}- permeable AMPA receptors in rat hippocampal slices. J Physiol (Lond) 491, 719-33.

Isaacson, J. S., Solis, J. M., and Nicoll, R. A. (1993). Local and diffuse synaptic actions of GABA in the hippocampus. Neuron 10, 165-75.

Itazawa, S. I., Isa, T., and Ozawa, S. (1997). Inwardly rectifying and Ca^{2+}-permeable AMPA-type glutamate receptor channels in rat neocortical neurons. J Neurophysiol 78, 2592-601.

Jonas, P., and Burnashev, N. (1995). Molecular mechanisms controlling calcium entry through AMPA-type glutamate receptor channels. Neuron 15, 987-90.

Jonas, P., Racca, C., Sakmann, B., Seeburg, P. H., and Monyer, H. (1994). Differences in Ca2+ permeability of AMPA-type glutamate receptor channels in neocortical neurons caused by differential GluR-B subunit expression. Neuron 12, 1281-9.

Kawaguchi, Y., Katsumaru, H., Kosaka, T., Heizmann, C. W., and Hama, K. (1987). Fast spiking cells in rat hippocampus (CA1 region) contain the calcium- binding protein parvalbumin. Brain Res 416, 369-74.

Kawaguchi, Y., and Kubota, Y. (1997). GABAergic cell subtypes and their synaptic connections in rat frontal cortex. Cereb Cortex 7, 476-86.

Kondo, M., Sumino, R., and Okado, H. (1997). Combinations of AMPA receptor subunit expression in individual cortical neurons correlate with expression of specific calcium-binding proteins. J Neurosci 17, 1570-81.

Kuriyama, K., Hirouchi, M., and Nakayasu, H. (1993). Structure and function of cerebral GABAA and GABAB receptors. Neurosci Res 17, 91-9.

Kyrozis A, Goldstein PA, Heath MJ, MacDermott AB (1995) Calcium entry

through a subpopulation of AMPA receptors desensitized neighbouring NMDA receptors in rat dorsal horn neurons. J Physiol (Lond) 485 :373-81

Labriola, A. R., and Laemle, L. K. (1977). Cellular morphology in the visual layer of the developing rat superior colliculus. Exp Neurol 55, 247-68.

Laezza, F., Doherty, J. J., and Dingledine, R. (1999). Long-term depression in hippocampal interneurons: joint requirement for pre- and postsynaptic events. Science 285, 1411-4.

Lambert, N. A., and Wilson, W. A. (1993). Discrimination of post- and presynaptic $GABA_B$ receptor-mediated responses by tetrahydroaminoacridine in area CA3 of the rat hippocampus. J Neurophysiol 69, 630-5.

Lane, R. D., Allan, D. M., Bennett-Clarke, C. A., Howell, D. L., and Rhoades, R. W. (1997). Projection status of calbindin- and parvalbumin-immunoreactive neurons in the superficial layers of the rat's superior colliculus. Vis Neurosci 14, 277-86.

Lane, R. D., Bennett-Clarke, C. A., Allan, D. M., and Mooney, R. D. (1993). Immunochemical heterogeneity in the tecto-LP pathway of the rat. J Comp Neurol 333, 210-22.

Langer, T. P., and Lund, R. D. (1974). The upper layers of the superior colliculus of the rat: a Golgi study. J Comp Neurol 158, 418-35.

Lee, P. H., Helms, M. C., Augustine, G. J., and Hall, W. C. (1997). Role of intrinsic synaptic circuitry in collicular sensorimotor integration. Proc Natl Acad Sci U S A 94, 13299-304.

Leranth, C., Szeidemann, Z., Hsu, M., and Buzsaki, G. (1996). AMPA receptors in the rat and primate hippocampus: a possible absence of GluR2/3 subunits in most interneurons. Neuroscience 70, 631-52.

Lo, F. S., Cork, R. J., and Mize, R. R. (1998). Physiological properties of neurons in the optic layer of the rat's superior colliculus. J Neurophysiol 80, 331-43.

Lu, X. Y., Ghasemzadeh, M. B., and Kalivas, P. W. (1999). Regional distribution and cellular localization of gamma-aminobutyric acid subtype 1 receptor mRNA in the rat brain. J Comp Neurol 407, 166-82.

Ludwig, A., Zong, X., Jeglitsch, M., Hofmann, F., and Biel, M. (1998). A family of hyperpolarization-activated mammalian cation channels. Nature 393, 587-91.

Mahanty, N. K., and Sah, P. (1998). Calcium-permeable AMPA receptors mediate long-term potentiation in interneurons in the amygdala. Nature 394, 683-7.

Mason, R., and Groos, G. A. (1981). Cortico-recipient and tecto-recipient visual zones in the rat's lateral posterior (pulvinar) nucleus: an anatomical study. Neurosci Lett 25, 107-12.

McBain, C. J., and Dingledine, R. (1993). Heterogeneity of synaptic glutamate receptors on CA3 stratum radiatum interneurones of rat hippocampus. J Physiol (Lond) 462, 373-92.

McCormick, D. A., Connors, B. W., Lighthall, J. W., and Prince, D. A. (1985). Comparative electrophysiology of pyramidal and sparsely spiny stellate neurons of the neocortex. J Neurophysiol 54, 782-806.

Misgeld, U., Bijak, M., and Jarolimek, W. (1995). A physiological role for GABAB receptors and the effects of baclofen in the mammalian central nervous system. Prog Neurobiol 46, 423-62.

Mize, R. R. (1992). The organization of GABAergic neurons in the mammalian superior colliculus. Prog Brain Res 90, 219-48.

Mooney, R. D., Klein, B. G., and Rhoades, R. W. (1985). Correlations between the structural and functional characteristics of neurons in the superficial laminae and the hamster's superior colliculus. J Neurosci 5, 2989-3009.

Mooney, R. D., Nikoletseas, M. M., Hess, P. R., Allen, Z., Lewin, A. C., and Rhoades, R. W. (1988a). The projection from the superficial to the deep layers of the superior colliculus: an intracellular horseradish peroxidase injection study in the hamster. J Neurosci 8, 1384-99.

Mooney, R. D., Nikoletseas, M. M., Ruiz, S. A., and Rhoades, R. W. (1988b). Receptive-field properties and morphological characteristics of the superior collicular neurons that project to the lateral posterior and dorsal lateral geniculate nuclei in the hamster. J Neurophysiol 59, 1333-51.

Moschovakis, A. K., Karabelas, A. B., and Highstein, S. M. (1988). Structure-function relationships in the primate superior colliculus. I. Morphological

classification of efferent neurons. J Neurophysiol 60, 232-62.

Nathan, T., and Lambert, J. D. (1991). Depression of the fast IPSP underlies paired-pulse facilitation in area CA1 of the rat hippocampus. J Neurophysiol 66, 1704-15.

Nicoll, R. A., Malenka, R. C., and Kauer, J. A. (1990). Functional comparison of neurotransmitter receptor subtypes in mammalian central nervous system. Physiol Rev 70, 513-65.

Okada, Y. (1992). The distribution and function of gamma-aminobutyric acid (GABA) in the superior colliculus. Prog Brain Res 90, 249-62.

Okada, Y. (1993). The properties of the long-term potentiation (LTP) in the superior colliculus. Prog Brain Res 95, 287-96.

Ozawa, S., and Iino, M. (1993). Two distinct types of AMPA responses in cultured rat hippocampal neurons. Neurosci Lett 155, 187-90.

Ozawa, S., Iino, M., and Tsuzuki, K. (1991). Two types of kainate response in cultured rat hippocampal neurons. J Neurophysiol 66, 2-11.

Pape, H. C. (1996). Queer current and pacemaker: the hyperpolarization-activated cation current in neurons. Annu Rev Physiol 58, 299-327.

Pasternack, M., Boller, M., Pau, B., and Schmidt, M. (1999). $GABA_A$ and $GABA_C$ receptors have contrasting effects on excitability in superior colliculus. J Neurophysiol 82, 2020-3.

Platt, B., and Withington, D. J. (1997a). Paired-pulse depression in the superficial layers of the guinea-pig superior colliculus. Brain Res 777, 131-9.

Platt, B., and Withington, D. J. (1997b). Response habituation in the superficial layers of the guinea-pig superior colliculus in vitro. Neurosci Lett 221, 153-6.

Saito, Y., and Isa, T. (1999). Electrophysiological and morphological properties of neurons in the rat superior colliculus. I. Neurons in the intermediate layer. J Neurophysiol 82, 754-67.

Santoro, B., Liu, D. T., Yao, H., Bartsch, D., Kandel, E. R., Siegelbaum, S. A., and Tibbs, G. R. (1998). Identification of a gene encoding a hyperpolarization-activated pacemaker channel of brain. Cell 93, 717-29.

Schiller, P. H., and Koerner, F. (1971). Discharge characteristics of single units in superior colliculus of the alert rhesus monkey. J Neurophysiol 34, 920-36.

Sivilotti, L., and Nistri, A. (1988). Complex effects of baclofen on synaptic transmission of the frog optic tectum in vitro. Neurosci Lett 85, 249-54.

Sparks, D. L. (1986). Translation of sensory signals into commands for control of saccadic eye movements: role of primate superior colliculus. Physiol Rev 66, 118-71.

Standen, N. B., and Stanfield, P. R. (1978). A potential- and time-dependent blockade of inward rectification in frog skeletal muscle fibres by barium and strontium ions. J Physiol (Lond) 280, 169-91.

Tokunaga, A., and Otani, K. (1976). Dendritic patterns of neurons in the rat superior colliculus. Exp Neurol 52, 189-205.

Wurtz, R. H., and Albano, J. E. (1980). Visual-motor function of the primate superior colliculus. Annu Rev Neurosci 3, 189-226.

Xu, T. L., Li, J. S., Jin, Y. H., and Akaike, N. (1999). Modulation of the glycine response by Ca^{2+}-permeable AMPA receptors in rat spinal neurones. J Physiol (Lond) 514, 701-11.